ACOUSTIC BUBBLE PROPULSION AND ROTATION FOR MEMS DEVICES

A Thesis

by

ONDER DINCEL

Submitted to the Office of Graduate and Professional Studies of
Texas A&M University
in partial fulfillment of the requirements for the degree of

MASTER OF SCIENCE

Chair of Committee,	Jun Kameoka
Co-Chair of Committee,	Laszlo Kish
Committee Members,	Aydin I. Karsilayan
	Kung-Hui (Bella) Chu
Head of Department,	Miroslav M. Begovic

December 2015

Major Subject: Electrical Engineering

ABSTRACT

The goal of this thesis research is to investigate acoustic wave actuated devices' abilities spatially in different media and with various designs. Self-trapped bubble oscillation generates cavitation at the open end of the micro channel under a continuous sound wave. The cavitation generates propulsion from the opening through to the end of the micro channel.

Researchers generally have found bubbles undesirable because of their non-linear effect in many applications. Therefore, there has been much research conducted in the area of eliminating the bubbles in liquid media. However, the use of bubbles can be beneficial in some applications like bubble powered actuators, switchers, and so forth. This research ensures the availability and feasibility of the bubble powered actuator for future medical applications.

In the current research, the actuator works with the principle of an oscillating bubble cavitation. The bubble cavitation and oscillation effect create a propulsion effect through the designed tubes. The captured bubbles generate force against to contact surface. The force against this force from the contact surface causes propelling. Different frequencies oscillate the bubbles in different lengths. Thus, the length of the bubble that is captured in the channel has an impact on the oscillation frequency by the sound wave, since the changes in lengths of the bubble also differ the oscillating frequency. In different oscillating frequencies can be used not only for a planar propulsion but also for bilateral and three dimensional propulsion. In addition, with various designs, a device

has an ability to substantiate many kind of motion in liquid media which means that propulsion effect can also use for circular or vortex motion purposes. In this research, up to 400 RPM circular and 70 mm/s instantaneous propelling speed are achieved in several designs by self-trapped and blocked micro-bubbles' oscillations under acoustic wave in water media.

In this novel study, availability and feasibility of acoustically oscillated micro-bubble based propulsion is demonstrated in spatial and rotational movement for future MEMS applications.

DEDICATION

All my works are dedicated to my family.

ACKNOWLEDGEMENTS

I would like to give my deepest gratitude to my advisor and committee chair, Dr. Jun Kameoka, who inspired and motivated me for my future scientific career. Without his guidance, I would not be able to study out with the MEMS. Thank you very much for his unlimited support, kindness, and patience. I would like to thank my committee co-chair Dr. Laszlo Kish for his support and his valuable Low Noise Electronic Design course. I would also like to thank Dr. Aydin I. Karsilayan for his advices that led me to find out my passion in scientific exploration. I would also like to thank my thesis committee member Dr. Kung-Hui (Bella) Chu for her supportive scientific analysis.

I am greatly thankful to my Bio and Soft MEMS lab mates, and my special thanks goes to Dr. Jun Zou for his Microelectromechanical Devices and System course, and my lab mates, Po-Jung Huang, Jaskirat S. Batra, Sina Baghbani Kordmahale, Jaligama Sravani for their extraordinary supports. I would like to thank to my colleagues Yusuf Dogan, Sinan Yigit, and Celal Bilgi for their valued knowledge and supports. My thanks also goes to Mrs. Sema Pulak for her advices and valued writing class. I also want to thank to my all other friends and colleagues and the department faculty and staff for making my time at Texas A&M University a great experience. I also want to extend my gratitude to the Turkish Ministry of Education for monetary support and giving opportunity me to have my master in science degree at Texas A&M University.

Finally, thanks to my mother and father for their encouragement and their advices. I also thank to my sister for her supports and to my wife for her patience and love.

NOMENCLATURE

3D	Three-Dimensional
BPM	Body per Minute
c	Speed of Sound
C	Celsius
CAD	Computer-Aided Design
CFD	Computational Fluid Dynamics
cm	Centimeter
Eq	Equation
dB	Decibel
f	Frequency
F	Force (Adhesion Force)
γ	Shear Strain
g	Gram
Hz	Hertz
I	Intensity
IPA	Isopropyl Alcohol
κ	Heat Radiation Constant
Kg	Kilogram
kHz	Kilohertz
L	Length

Lab	Laboratory
μ	Dynamic Viscosity
μm	Micron
m	Meter
mg	Miligram
MHz	Megahertz
mm	Milimeter
MEMS	Micro Electro-Mechanical System
N	Newton
NNR	Noise Reduction Rating
P	Pressure/ Power
ρ	Density
Pa	Pascal
PC	Personal Computer
PDMS	Polydimethylsiloxane
PP	Polypropylene
R, r	Radius
Re	Reynolds Number
RPM	Revolutions Per Minute
s	Second
σ	Surface Tension
t	Time

τ	Torque
T	Period
U	Velocity
UV	Ultraviolet
ω	Angular Frequency
W	Watt
v	Kinematic Viscosity
V	Volt
z	Acoustic Impedance

TABLE OF CONTENTS

Page

LIST OF FIGURES

Page

LIST OF TABLES

Page

1. INTRODUCTION

1.1 Objective and Motivation

Many researches and designs have been made and represented about micro swimmers in literature for medical and scientific research purposes. Micro swimmers, in literature, generally are focused on biomedical uses.

Scientists believe that emerging technologies in micro swimmers will give an opportunity to perform micro surgeries, drug deliveries, and many other medical purposes. For instance, a patient, who was gone blind by diabetes, can have a contactless and harmless microsurgery by micro swimmers. Micro swimmers can reach the retina of patient through the vitreous body to discard the reasons for unclogging plaque or atheromas in blood vessels. These examples can be extended. However, swimmers require some crucial characteristics to perform future medical implementations. The ability of remote control and non-contact drive are highly desired in medical experiments and researches for micro swimmers. [1] Nevertheless, biocompatibility and non-toxicity are the first required characteristics of a medical swimmer. Medical developments motivate researchers to create efficient, non-toxic, easy to implement, biocompatible, contactless micro swimmers. Several techniques, which are magnetic[2-4], chemical reaction[5-7] as well as biological mechanism based[8-10], and various other techniques[11, 12] using micro swimmers have been practiced in different media and scales. Researches achieved the propulsion magnetic[2], catalytic[6, 13, 14], propulsion by bacteria[8], and so forth. Literally, propulsion is not enough for leading a material or device to a specific place in liquid media. Thus, a device which has turning

and rotating abilities with an efficient propulsion characteristic in micro scale is required. Applications and researches show that many techniques can be applied to a device to get the required propulsion with a rotating ability. Nevertheless, many of them are insufficient in terms of three dimensional controlling and dealing with scallop theory. [15] In scallop theory, to generate propulsion, the device need to have irretrievable motion, such as corkscrew and oar motions. [16]

Beyond all existing techniques, bubble oscillation based micro swimmer has the advantage of propulsion ability in different directions and in various liquids. In terms of different liquids, the device can be operated remotely in highly toxic environments, organic or inorganic media. The contactless acoustic bubble excitation in different oscillation frequencies gives the bubble empowered device an opportunity to move in different directions. Bubbles have an ability to oscillate in certain frequencies. Within oscillation frequencies, bubbles create expanding and shrinking behavior. Expanding and shrinking phenomena create a cavitation in an open-ended tube. It is going to examine and represent in oncoming sections.

1.2 Small Scale Propulsion

In micron scale dimensions of a swimmer means that it has small Reynolds numbers. Thus, inertial forces can be lower than viscous forces.

$$Re = \frac{\rho UL}{\mu} = \frac{UL}{\nu} = Inertial\ forces/Viscous\ forces \quad (1.1)$$

Where ρ is density of fluid (kg/m^3), U is velocity, μ is the dynamic viscosity (kg/m s) L is the typical dimension of the system (μm), and v is kinematic viscosity (m^2/s). According to the Eq. 1.1, when the Reynolds number is very small for a micro

swimmer, in non-viscous water, viscous forces becomes dominant. [17] In this manner the liquid media is also important for estimation of propulsion and feasibility of an application. Human blood, which is viscous, is the most desired liquid media for the applications. Therefore, the applications usually test in viscous liquids. Generally, for the millimeter and centimeter scale swimmers the Reynolds number is around hundreds. In many applications the researcher tends to neglect the viscous forces. However, in micro scale and nanoscale, the viscous forces become dominant. In addition, Reynolds number can be calculated or estimated by the actuator dimensions not by the size of the total device.

In addition, Brownian motion becomes dominant in micro and nanoscale environments. Brownian motion is a non-predictable molecular based motion which effects propulsion and direction of propulsion negatively. Because of the existence of Brownian motion effect, it is very hard to design nanoscale and also very small micro scale swimmers. Brownian effect is very hard to avoid because it is kind of noise of a system that caused by the temperature.

2. ACOUSTIC WAVE

2.1. Wave Characteristics

Sound waves are periodic pressure changes in molecule size of a media. While the sound wave is propagating in the media, the media does not move. The modelling of a sound wave is not transverse wave because the propagation of sound is parallel to the motion of sound which is a longitudinal wave. Typically sound's speed is in air 340 m/s, in water 3000-5000 m/s, in steel 8000 m/s. Over 20 kHz generally calls as ultrasonic, under 20 kHz calls as acoustic. Acoustic waves usually call as a human hearing sound waves. However, ultrasonic waves are over 20 kHz which are not hearable by human. The wave of sound is a form of the mechanical energy on the media. Vibration or any impact can easily create a wave in a media. This mechanical phenomena travels through media or interact with barriers. Mechanical effect creates resonance. Thus, the media and the materials that are used can determine the behavior of a wave. [18] To investigate the sound, vibration requires for sensing or generating sound like in human ears. Human ears' drums can hear mechanical vibration. Ear drums are the well-made natural transducer. To sense, the sound wave should be enough resolution. As an example, speed of sound in water three times more than sound in air, therefore to have same degree of resolution, three times more higher frequencies should be in water. [18] Below 1 Hz frequencies generally call as infrasonic waves. They can be produced by explosion, earthquakes etc. Wind currents in atmosphere produces infrasound waves, some animals can sense the wind sound wave. Therefore, they can sense earthquakes, upcoming storms, and so forth. Wind turbines produce high frequency wind waves. Therefore, they

are hearable by humans and create discomfort for distant residents. The way to explain the sound wave propagation is to consider the wave as pressure waves. Particles in the media can effect by the pressure waves with different levels. Particle velocity is the highest in non-displacement point of the pressure field, and it is the lowest velocity in the rarefaction and compression peaks [18]. To know the speed and sound wavelength is very crucial for the applications of acoustic actuators.

$$c = f\lambda = \frac{\omega}{\kappa} \tag{2.1}$$

From the Eq. (2.1), it is easy to calculate wavelength with the speed if we know the frequency. The speed of sound (c) is 344 m/s at 1 atmosphere and 20 °C in air and 1480 m/s in water. With the Eq. (2.1), it is easy to estimate linear sound wave propagation in media. To investigate the non-linear propagation of sound wave in media, we need to investigate the speed and pressure in terms of particle dimensions.

Intensity of a wave is one of the most important characteristic for affecting a receiver or actuator. The distance from the source changes the intensity. Going away from the source diminishes intensity. The phenomena occurs in many type of waves for example acoustic wave which has spherical propagation into a media.

Wave has important characteristics such as acoustic pressure, reflection of wave, acoustic impedance, acoustic intensity, and attenuation. Velocity of an acoustic wave pressure can be effected by the medium with its acoustic impedance. To illustrate, thinking current as a velocity, and pressure as a voltage. The impedance in acoustic wave can be found by the velocity and pressure. Every material has their own acoustic impedances [18, 19].

	Air	Water
Density (kg/m^3)	1.2	1000
Speed of Sound (m/s)	340	1480
Acoustic Impedance (kg/m^2s)	400	1.5×10^6
Attenuation (dB/m)	1200	0.22

Table 1: The Acoustic Wave Propagation Characteristics of Air and Water [10, 11].

It is obvious that speed of sound and acoustic impedance of water are significantly higher than air in Table 1. According to the ratio of attenuation and acoustic impedance of air and water, sound wave has better propagation in water media relatively to air.

2.2. Sound Wave in Liquid

When sound wave applies into the liquid, density change occurs. Changes in liquid density are negligible for linear approach. However, if the density fluctuation is very high, the wave speed will act in non-linear manner. When the speed of the particle is highest in non-displacement wave changes, Brownian motion becomes dominant in micro and nanoscale environments. Brownian motion is a non-predictable molecular based motion which affects propulsion and direction of propulsion negatively. Because of the existence of Brownian motion effect, it is very hard to design nanoscale and also very small micro scale swimmers. Brownian effect is very hard to avoid because it is kind of noise of a system that caused by the temperature.

Acoustic impedance of water and air are important for to determine the sound pressure level .While estimating the pressure level hydrophones can be used for liquid media to calculate the impedance. After assuming that pressure equilibrium, no attenuation with very low viscosity, and no heat transfer the acoustic impedance becomes: [18]

$$z = \rho c \tag{2.2}$$

Where ρ is density of media (kg/m^3), c is speed of sound wave in media (m/s). The Eq. (2.2) is very simplified and linear because non-linear effects did not counted. Acoustic pressure divides into particle velocity gives the acoustic impedance. However, time varying and non-linear effects change the velocity.

Intensity of sound is another characteristics of sound waves. Intensity of sound is generally known as loudness. It shows the energy level of the sound. The energy spreads in a media with spherical motion and reduces the initial intensity with expanding level of the energy. Figure 1 visualizes the phenomena.

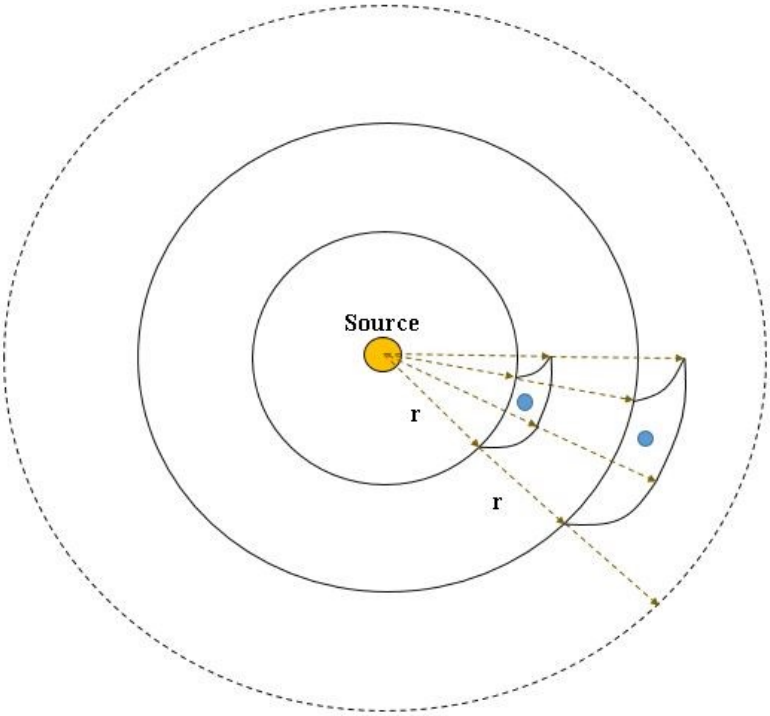

Figure 1: Intensity of Sound at Different Distance Levels

The blue dots in Figure 1 at different levels represent same integration area. The area is same whereas the intensity is decreasing. The total intensity is equal at the surface of the every energy level that are shown in the figure. The basic intensity equation, which is given Eq. (2.3), represent a fundamental sense of the power level knowledge related to the distance changes.

$$P = 4I\pi r^2 \tag{2.3}$$

Equality is also related with no attenuation into signal amplitude. With assumption of no attenuation at any levels bubble oscillation amplitude can be precisely calculated. However, materials have their intrinsic molecular characteristics that can cause high or low loss at the strength of the acoustic wave. Total energy density times

the speed gives the intensity. Total energy density can be found by the kinetic energy theorem with assuming mass is directly density and speed is the first harmonic of the displacement. According to the plane structure of a wave with having acoustic impedance equation, the sound wave intensity at x-y plane can be found by; [18]

$$I = \frac{P_A^2}{2Z} \tag{2.4}$$

To understand bubble action in water media, the general equation which is Eq. 2.4 or any approximation may not meet with the reality when the sound field is calculated. The sound field should be measured by hydrophone. In addition, hydrophone should be smaller acoustic wavelength for correct measurement.

Attenuation is also another issue for the sound waves in liquid media. Because viscous forces will increase the attenuation in liquid media, and another attenuation reason is the heat flow that occurs in the media molecules motion. Increasing the frequency means the increasing the attenuation by the factor of square value of frequency. [18] Acoustic wave propagation into liquid media and solid structures have some nonlinear characteristic. [20] Further investigations and research should be done in soundwave interaction at the surface of a material.

Acoustic sound waves' pressure spatial propagation in air, water or any other gas and liquid media can be determined by Eq. 2.5 [21]:

$$\Delta p = \frac{\partial^2 p}{\partial x^2} + \frac{\partial^2 p}{\partial y^2} + \frac{\partial^2 p}{\partial z^2} = \frac{\frac{1}{c^2(x,y,z)}\partial^2 p}{\partial t^2} \tag{2.5}$$

2.3. Piezo-ceramic Transducer

Piezoelectric transducer can change pressure to voltage or voltage to pressure that can create sound. In my thesis, increasing the voltage the sound pressure will be increased. In addition to this, piezoelectric transducers can also use for measuring the physical effects that on piezo electric material can be sensible as a voltage change by the transducer.

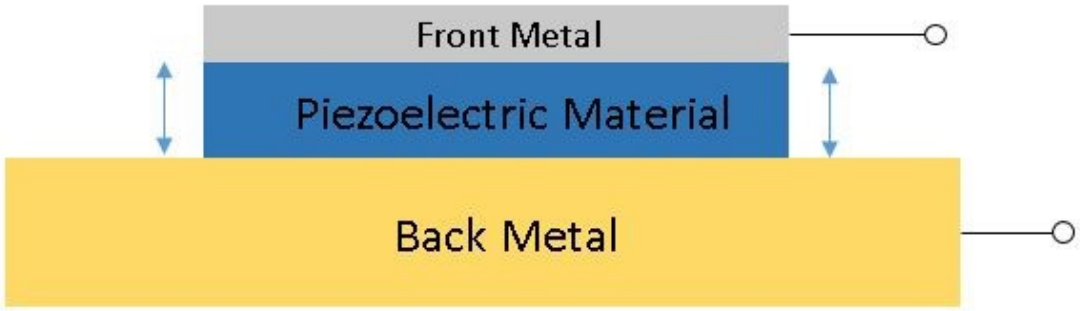

Figure 2: Piezoelectric Transducer Basic Structure

As it seen from the Figure 2, a piezoelectric transducer has a front metal as positive pole and back metal that has negative pole. Square wave or sinusoidal wave can create sound wave through the vibration between metals by piezoelectric material. Piezoelectric material produces pressure by the applied voltage. Then, the sound occurs similar with the applied frequency from the electric source.

The used piezoelectric transducers have 20 mm, 24 mm, and 30 mm external diameters and their operating voltages are 10 V, 10 V, and 12 V. The transducer's function is known as a piezoelectric diaphragm. Different diameters applied because of for 3D motion bigger surface required to observe continuous effect. The acoustic and

ultrasonic waves, which are used for thesis, are generated by the piezoelectric diaphragms.

3. BUBBLE

3.1. Free Bubble Oscillation

For stationary, bubble in liquid has a pressure of gases that captured or included in. The liquid pressure at bubble wall and inner side surface tension pressure which is Laplace pressure can be found by:

$$P_\sigma = \frac{2\gamma}{R} \tag{3.1}$$

Where γ is surface tension, and R is the radius of a spherical bubble. According to the Laplace pressure theory and the Eq. 3.1, surface tension is an important criterion to estimate the inner pressure at interacting with liquid media. A stationary bubble has a typical effect when the acoustic wave applied. The acoustic wave is a pressure based wave that can affect the shape of the bubble while it passes beyond the bubble. Thus, the media is very important for the gas oscillation. Because bigger surface tension effect will require higher pressure for having better oscillation and cavitation.

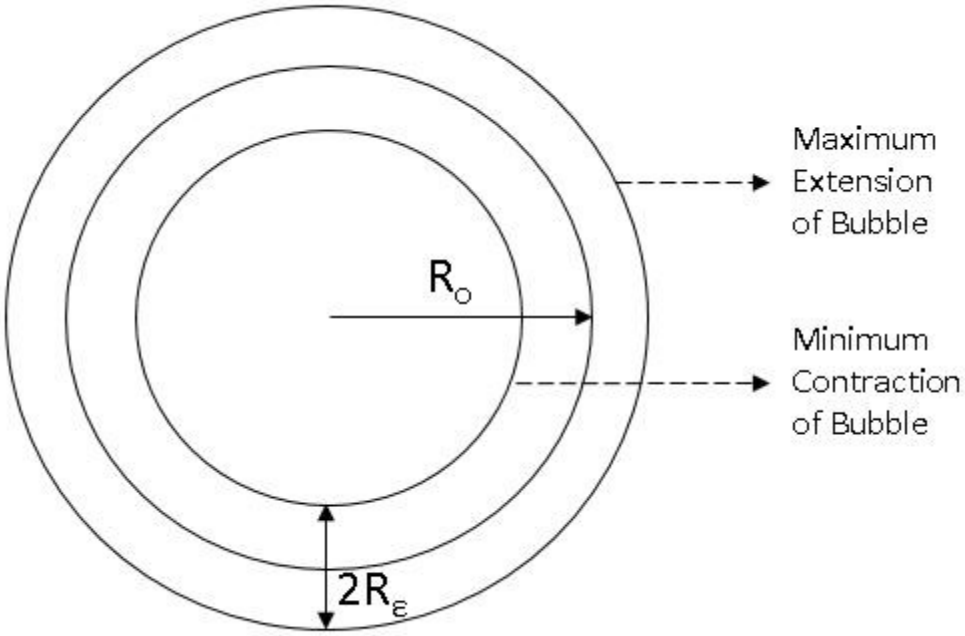

Figure 3: A Bubble Extension and Contraction While Oscillating

According to the Minnaert bubble oscillation frequency theory, bubble wall has a motion for bubble radius. [22] A bubble extension and contraction changes represented by Figure 3 and the related equation which is:

$$R = R_o + R_\varepsilon(t) = R_o - R_\varepsilon e^{i\omega_o t} \tag{3.2}$$

From the equation 3.2 Minnaert bubble oscillation frequency can be calculated with the bubble radius change in integration and the pressure values that applied by spontaneous air bubble, atmospheric pressure, and media pressure. However, the surface tension should be negligible, which is represented by:

$$\omega_o = \frac{1}{R_o}\sqrt{\frac{3\kappa p_o}{\rho}} \tag{3.3}$$

Which equals to:

$$f_o = \frac{1}{2\pi R_o}\sqrt{\frac{3\kappa p_o}{\rho}} \tag{3.4}$$

In the Eq. (3.3) and (3.4), κ is assumed as a constant that caused by the heat radiation from the bubble. κ generally has a value around 1 to 1.4 according to the temperature of a media. R_o is the radius of a bubble, and p_o is the hydrostatic pressure of a liquid at bubble sphere. ρ is the density of media. The most simplified version of bubble oscillation estimation can be found by the Eq. (3.5) for water media after basic calculations: [22]

$$R_o f_o \cong 3Hz\ m \tag{3.5}$$

3.2. Bubble Oscillation in Tubes

Bubble oscillation in tubes is fairly different from the free bubble oscillation. The logic behind oscillation does not change, however the action of the bubble changes. Thus, new equation will be required for the estimation of bubble oscillation frequency in tubes.

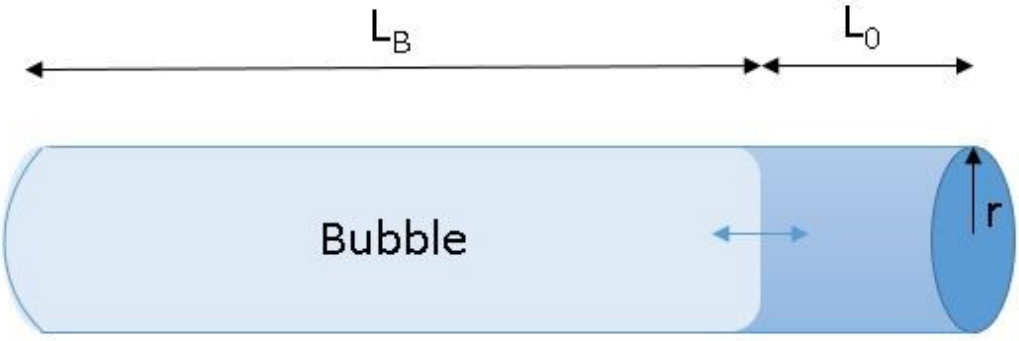

Figure 4: Captured Bubble in a Tube

According to the Oğuz and Prosperetti: [23]

$$f_o = \frac{1}{2\pi}\sqrt{\frac{\kappa P_o}{\rho(L_o + \Delta L)L_B}} \tag{3.6}$$

Where L_B is the length of a captured bubble in tube, and L_o is the length of the remained part of a tube from the bubble end to orifice of the tube as it seen in the Figure 4. ΔL is end correction of the encapsulated bubble. For calculations, encapsulated bubble end correction can be found by:

$$\Delta L = 0.6133r \tag{3.7}$$

The related oscillation frequency can be found by the Eq. (3.6) and (3.7). The approximation to the original natural bubble oscillation frequency is better in Eq. (3.6) instead of Eq. (3.4).

3.3 Adhesion Force of a Bubble

The principles of a different materials interaction can be chemical, electrical, and physical. One of the most important force for a stationary bubble on the surface of a material is adhesion force. This force keeps a bubble hold on the surface of a material. If any forces such as cohesion, buoyancy, propulsion and so forth is bigger than the adhesion force, the bubble will be disconnected from the material surface or dragging effect will be seen. The intrinsic and/or extrinsic forces' direction and projection affect the disengagement of a bubble from a surface. However, instead of many forces effects on a bubble, in free bubble oscillation inside a cage has an interaction on the inside

surface of the design. The occurrence of adhesion force inside of a design while the bubble expanding and shrinking creates reverse force to balance the adhesion forces.

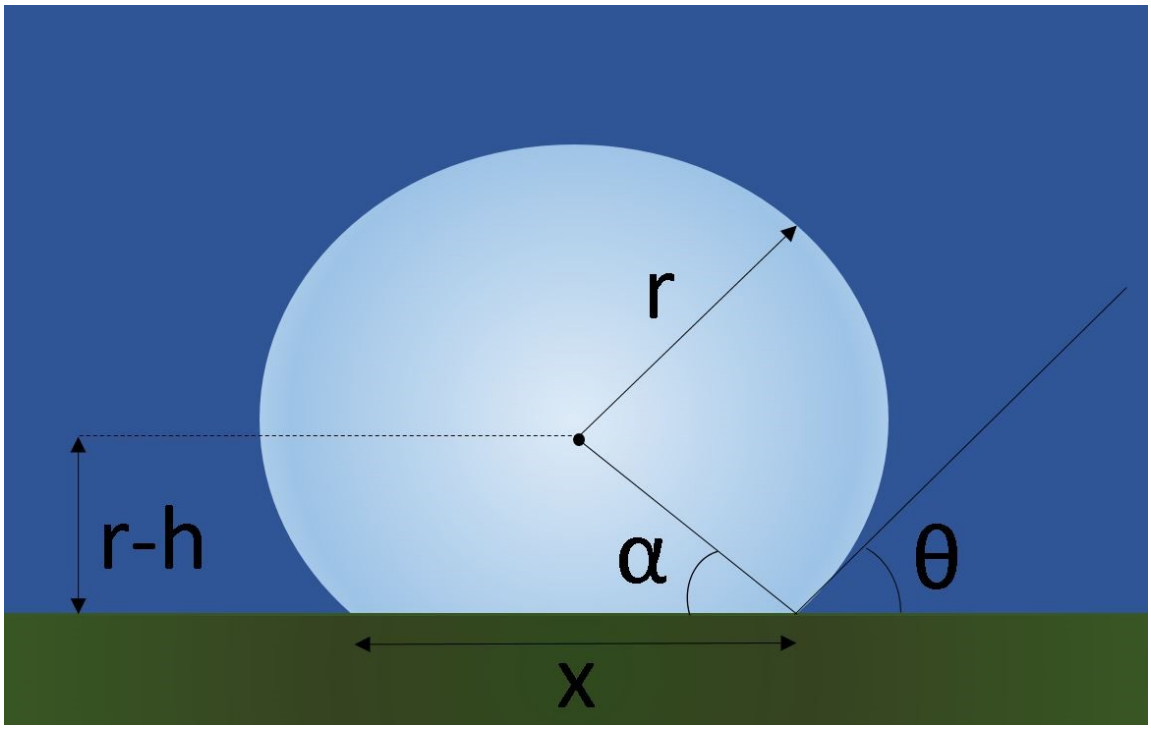

Figure 5: A Bubble Contact Angle and Adhesion Force

Related adhesion force formula is given by

$$F = \pi x \gamma sin\theta \tag{3.8}$$

in which γ is shear strain of the bubble, θ is contact angle, x is the diameter of the bubble surface contact area.[24]. The formula 3.8 is going to use to calculate the adhesion force of the surface. In addition, Figure 5 is going to use to determine the contact angle of a bubble at the surface of material such as resin and PDMS.

The force and pressure, which occur when a bubble oscillating into the designed device, are given in the figure 6.

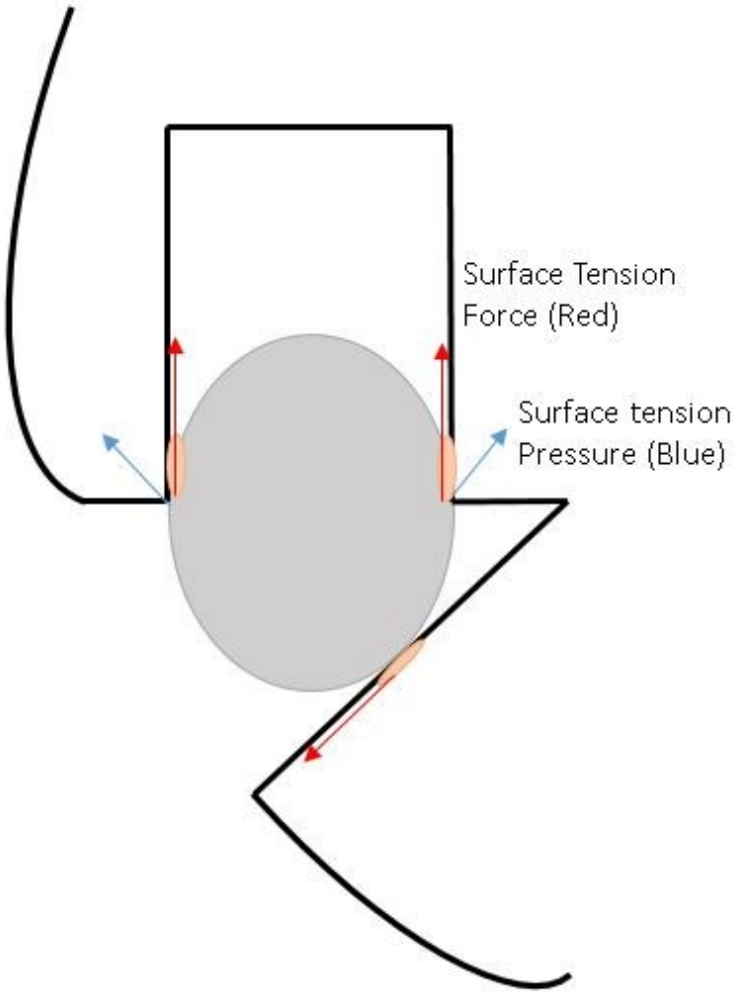

Figure 6: The Captured Bubble Oscillation Created Forces and Pressures

As it seen in the Figure 6, surface tension pressure of the bubble creates forces while oscillating. Moreover, the parallel component surface tension forces' at the bubble-device contact faces which are represented as red arrows generate reverse forces. The reverse forces cause of the spinning and/or pulling effects.

4. SIMULATIONS

4.1. Simulation of a Sound Wave Pulse in Water

This theoretical simulation is for understanding the wave pulse propagation in water media. Before having experimental setup the soundwave effect on a vessel or a closed container should be explored. Peak points and unwanted reflected waves existing places should be determined.

The simulation is for understanding sound wave pulse propagation in water media into a container. To visualize and to estimate the acoustic wave distribution in water media, and in the limit of the water tank, I have used the acoustic wave radiation in water media phenomena Eq. (2.4). The related Matlab source codes are given in Appendix B.

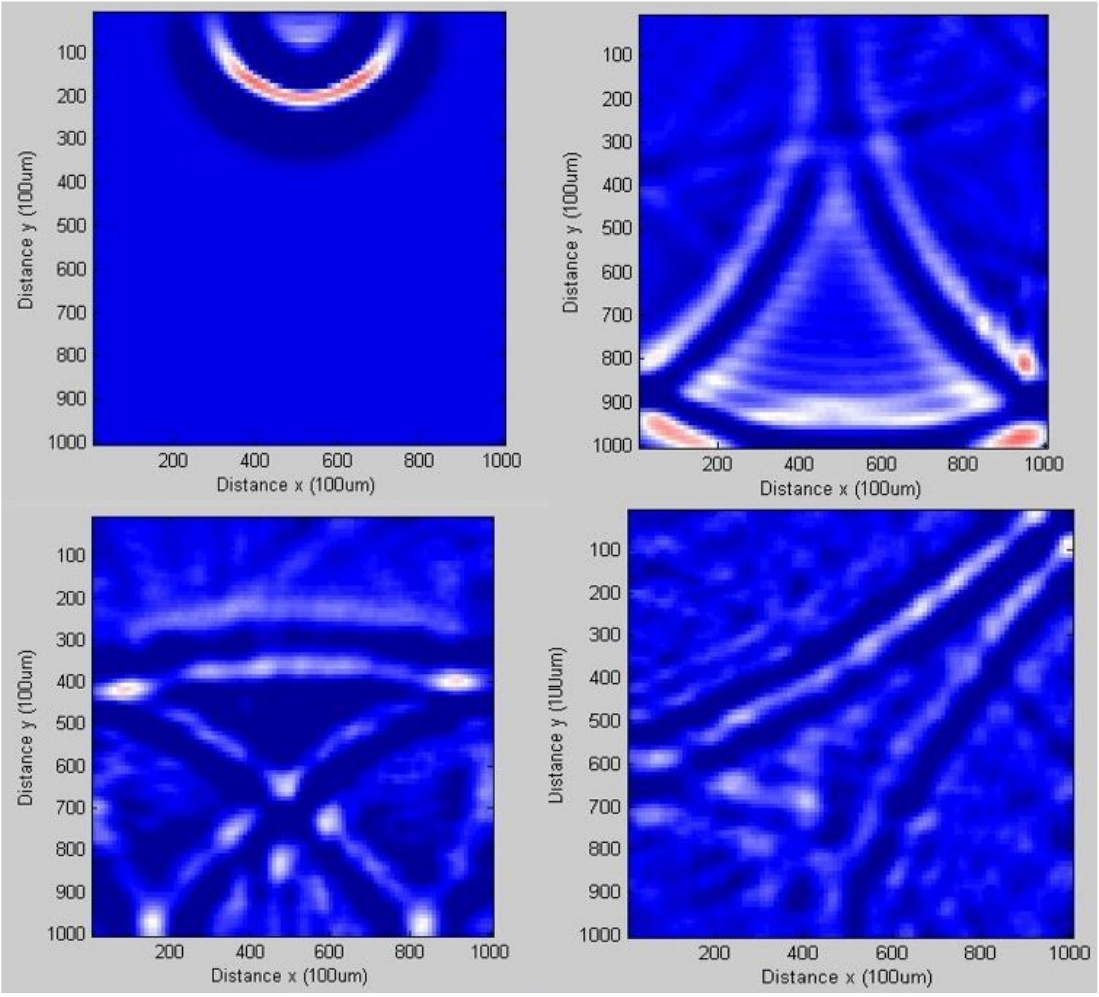

Figure 7: The MATLAB® 2014a Simulation of a Soundwave in Liquid in z Direction Vision in the Boundary Condition of Experimental Setup

According to the Figure 7, red waves represent the peaks of the sound wave in liquid media. From the simulation, to understand the sound behavior into a vessel investigation of the returning sound wave peaks is crucial. Because, the returned waves will create inconsistency in terms of oscillating bubbles into my designs as it seen in the figure 7. According to the simulation, the designs should not be located at the corners or closed to the corner points.

4.2. Flow at Microfluidic Channel Simulation

Acoustic mixing device, which is represented at fabrication and testing sections, has a function actively mixing two different liquids.

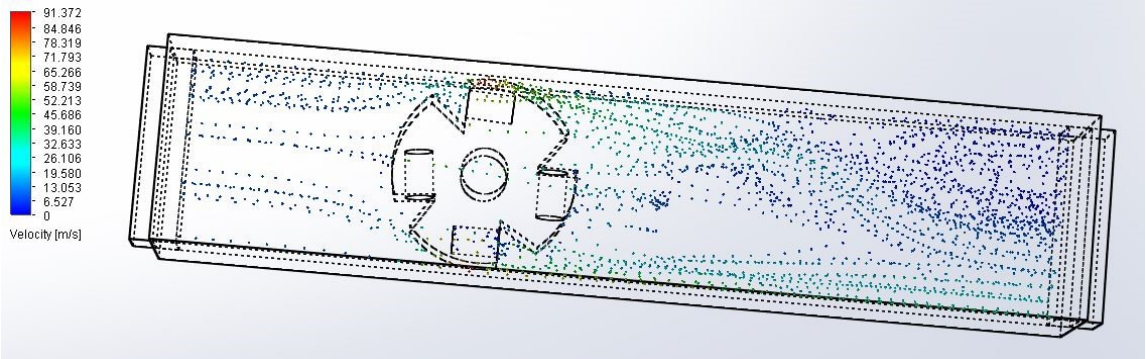

Figure 8: Flow Pattern at the Designed Testing Microfluidic Channel with the Device Blocking

According to the passive flow action in the simulation, the flow is laminar in the beginning after block of the mixing device the Reynolds number higher changes occurs as vortex. However, even vortex occurrence and other effects do not have a significant effect on mixing. As it is seen in the Figure 8, closefitting points have high velocity. After high velocity the released hydraulic pressure can be seen. Furthermore, the laminar flow pattern has no significant changes. The design allows not only the purpose of mixing but also back and forth motion is available for future applications. Nevertheless, the design remains stationary for the observation of mixing effect.

Testing the design and device at a computational fluid dynamics program gave an opportunity to observe the fluid flow in real world conditions such as ambient temperature, air pressure, and hydrostatic pressure. Air pressure adjusted to the regular atmospheric pressure as 101325 Pa. Experiment place and water temperature is assumed

that having 20° C. Hydrostatic pressure is assumed zero because the testing tube do not have a significant height. According to the simulation results, putting the device directly to the microfluidic channel creates a problem in terms of flow rate. Therefore, turbulent flow occurs after couple mm later from the device. To avoid this problem, the microfluidic device should be designed in figure 9 or in similar designing technique.

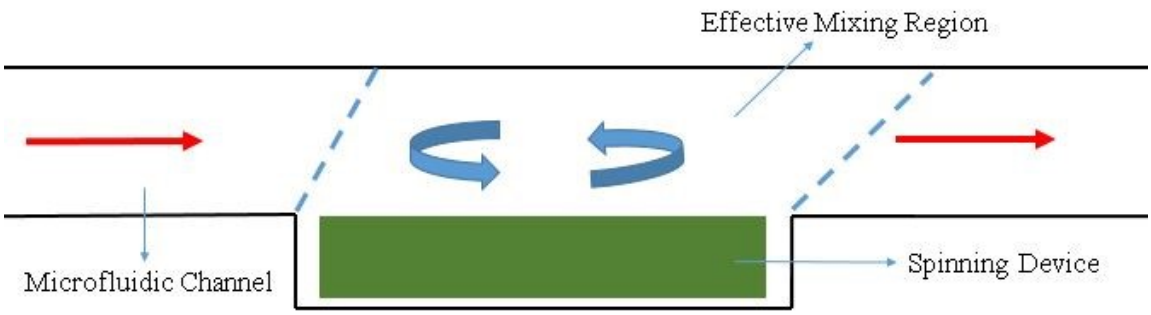

Figure 9: Microfluidic Mixing Device Channel Side View

As it seen in Figure 9, the spinner should be placed a pocket that suitable for operating. Effective mixing region is affected by the flow. Whirling mixing pattern will be occurred as a pulled form.

5. MICROFABRICATION AND EXPERIMENTAL SETUP

5.1. Microfabrication Process

For microfabrication I have used a 3D Micro printer which has 25 um resolution. Highly precise optical system used for light system can penetrate 16 um resolution with stereolithography process. UV-light has been used for penetration of the material through the surface to build layers. A special material which has UV light absorbents uses for building the structure. The special resin has been used for fabricating the devices. The design and printing steps are;

1- Calculations and Draft

2- Drawing in a CAD program

3- Micro Printing Process

4- Cleaning and Curing Process

5- Further Cleaning and Curing for PDMS based materials.

6- Microfluidic Channel and Testing Device Setup and Assemble.

Figure 10: Process of Micro-Fabrication

As it seen in the Figure 10, process includes 6 main steps which are explained herein below with details.

1- Calculations and Draft: Before using a CAD program, considering minimum resolution and curing process limitations the design will be calculated with its center of gravity and boundary conditions.

2- Drawing in a CAD program, SolidWorks® 2014 used for design process. The designs have been saved as .stl format to be recognized by other 3D printing programs.

3- Micro printing process starts with regulating a design in magic software. Fixing the design and designing faults can be completed by the Magic Software®. Rotation of the device and supports creation are made by the program. Supports are

required for curing and taking off the device more effectively. The convenient and more reinforced supports have been selected and applied. After generation of support the next program requires for creating micro-printer recognized photo files. Afterwards, Perfactory RP® Program creates the picture of layers into a file for uses of printer. Every single layer is created as a picture around 25 to 35 micron resolution. Then, Micro Printer® Program is used to start the printing process. Light engine and positioning the stereolithography machine are made by the program. With uploading and pouring the resin material the printing process starts.

4- Cleaning and Curing Process: The printed device should be takeoff from the steel platform as soon as possible otherwise the remained resin into channels will be dried. After taking off step, the printed design should be cleaned into isopropanol or ethanol solution for cleaning the residues into channel and around device. After cleaning curing with UV light is mandatory for hardening and strengthening the design. EnvisionTEC® UV light exposure machine is used for curing.

5- Further Cleaning and Curing Process: A mold fabrication by the micro-printer has same steps in fabrication. After all, PDMS material used designs have extra steps to fabricate. The first step for creating liquid PDMS solution is mixing 10 times more liquid dimethylsiloxane into 1 unit silicone elastomer. After mixing process, the second process is to remove bubbles with applying high pressure. While removing the bubbles the mold should be coated with silane layer with vaporing the material in a closed vacuum system. After removing the mold from the vacuuming the liquid PDMS should pour to the mold. The PDMS poured device also requires to remove bubbles with

applying high pressure again. After removing all bubbles, the mold should put into an oven for 3 hours at 65° C.

6- Microfluidic Channel and Testing Device Setup and Assemble: After step 4 the device should have extra practices to perform a microfluidic device. For creating a microfluidic device molding and curing PDMS steps are given in the step 5. To assemble the complete device the PDMS molds should be put into oxygen plasma machine to bind together the layers. Before applying plasma effect to the tap layer of PDMS molds, they need to be sure about cleaned by IPA at an ultrasonic cleaner. After plasma binding the device should cure at an oven. In this step, provided pumps and/or testing environment should be provided and performed. Experimental data was collected in this step.

5.2. Experimental Setup

The typical experimental setup is given below. The function generator is Rigol® DG102, and the high voltage amplifier is Trek® model 2210 which has 100 times amplification. Fluke® 8846 precision multimeter used for measuring the impedance and high voltage values. Tektronix® TBS1202B oscilloscope is used for observing the frequency changes that related to signal generator. The lead free 10 V 20 mm and 24 mm ceramic piezoelectric transducer are used in testing. While having experiments 3M® disposable ear plugs which have NNR 32 dB and 3M® Tekk Folding Ear Muffs which have 23 dB NNR are used to protect from eardrum deformation. 3M® safety googles are used for reduce the sound effect on cornea. The testing setup is shown in the figure 11.

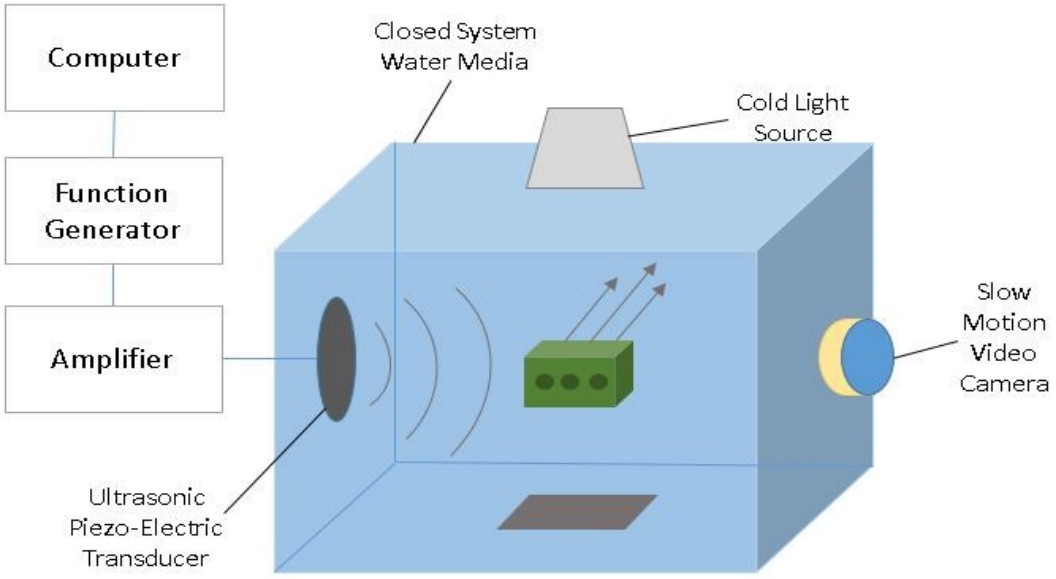

Figure 11: Experimental Setup for Acoustic Scallop Theory Based Designs

The piezoelectric transducer was placed at the sidewall of the container as it seen in Figure 11, because the research papers that we took as a starting point and reference are used to put the transducer at the sidewall of the container [25-28]. As a cold light source, power LED was used to illuminate the testing and focus on the device. Cold light source is required for not causing an additional temperature effect. The transducer and oscillation have their own temperature effects in the container. Computer has used for to shifting the frequency and different amplitudes by time domain in the testing program of the function generator in the PC. Slow motion video camera is used for to count the RPM. Ultrasonic piezo-electric transducer placed at the side and also at the bottom of the container in some experiments. Sinusoidal signal from the function generator is used for to generate acoustic wave in different frequencies. In some of my experiments, we have

used square wave instead of sin wave, because low voltage levels in sin wave the generated waves were not as strong as square wave generated acoustic waves. In spite of the fact that, in high voltages amplifications, the square wave source can cause a failure at piezo-electric transducer.

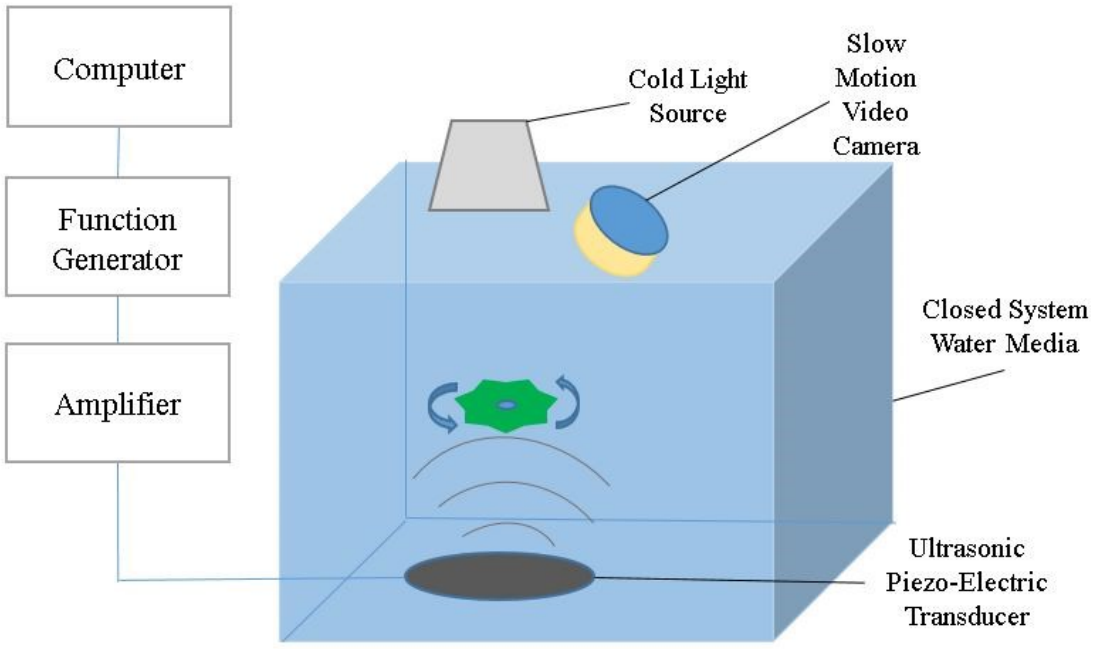

Figure 12: Experimental Setup for Restrained Bubble Designs

According to Figure 12, the piezo electric transducer is locater under the testing vessel. Rotating device has worked more efficiently than the sidewall piezo-electric transducer installation because of the distance effect that is represented at the results section. Rotating device is rotating at different level of water with various frequencies. The changes with hydrostatic pressure are represented and evaluated at the results

section. Closed system water media has many different material based containers related with the application. Several designs with their explanations are given at section six.

6. DESIGNS, TESTS, AND RESULTS

6.1. Designs, Test and Results for 3D Micro-Tube Bubble Propulsion

Many devices are designed and tested in this section. However, none of them is worked because of the resin and PDMS inconsistent behavior when applying acoustic wave. The designs are calculated and drawn according to the Equation 3.6. According to the calculation the related sizes are designed L= 500 µm, 120 µm wide. The calculated and expected bubble oscillation frequency is 7.9 kHz. The gas pressure according to the liquid pressure is around 174 Pa for 0.018 m high in the tank to the gas for the calculation.

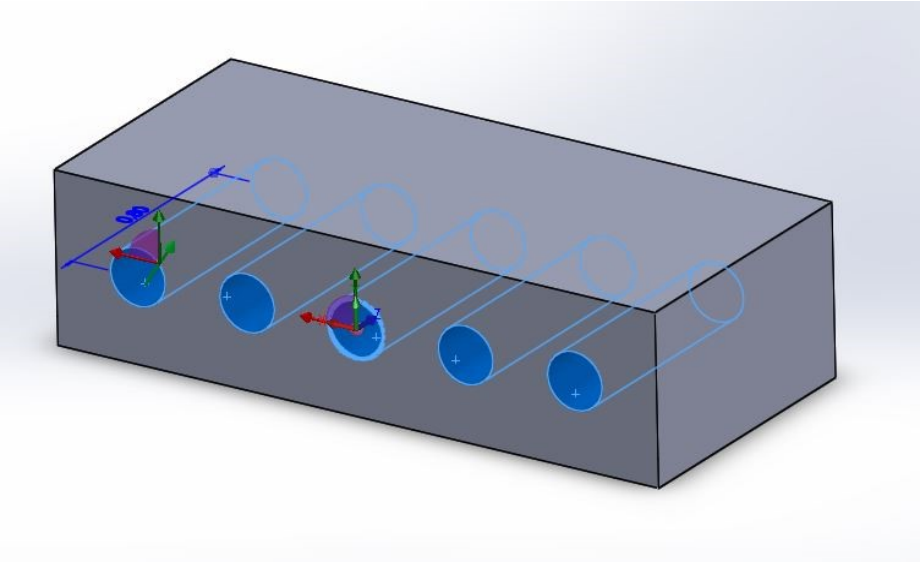

Figure 13: The First Design that has the Smallest Dimensions that can be Achieved by the 3D Printer [27]

As it seen in the Figure 13, the dimensions of the design are 2000 x 900 x 500 µm which are the smallest dimensions that was allowed to design by the 3D printer in terms of the horizontal and vertical resolution.

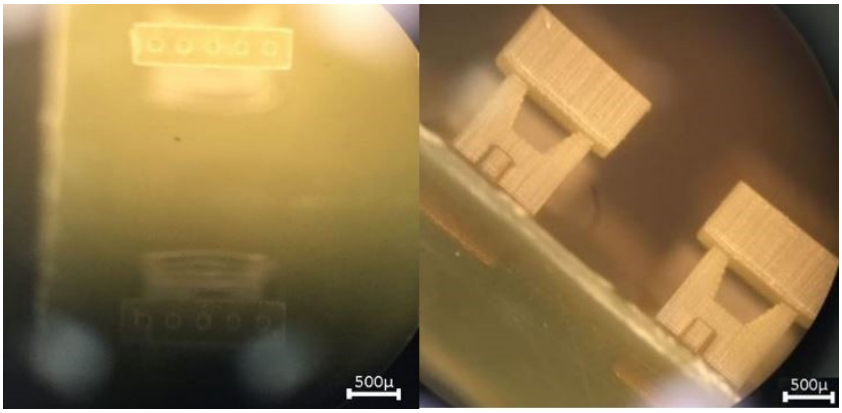

Figure 14: The Fabricated and Tested Device Top View and Side View Respectively

The fabricated device top view and side view with its supports seen as in the Figure 14. After no effective motion, another design are made and tested. Designs have several lengths and sizes. The bubbles of different sizes oscillate at different frequencies. Therefore, to say which design is active in what frequency, it is crucial to know the size of trapped bubble in advance. Thus, the trapped bubble frequency is determined via a simple mathematical volume calculation, by using the formula that mentioned sin the introduction. According to the formula, the fallowing devices had to oscillate around 7.2 kHz, 4.5 kHz, and 10.4 kHz respectively.

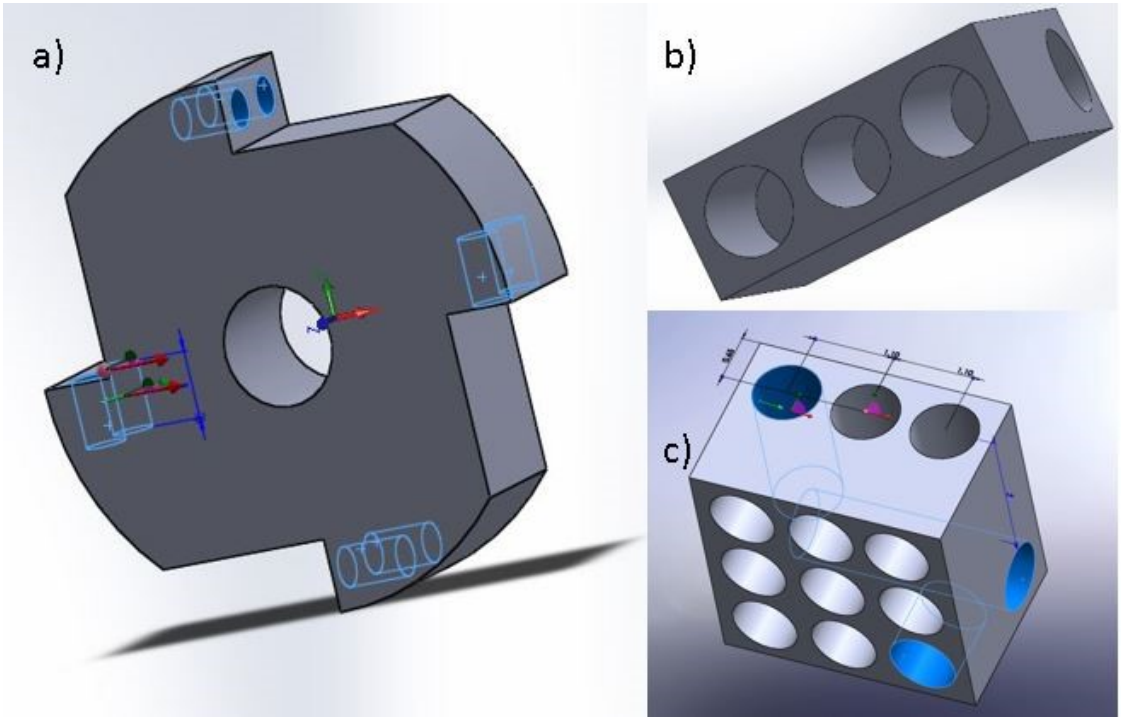

Figure 15: Different Studied Designs for Bubble Oscillation

The designs given in the Figure 15 did not react. To determine the oscillation frequency of the captured bubbles, all designs were scanned between 500 Hz and 30 kHz with 100 Hz increments. Bubbles that are trapped inside of a tube, at various frequencies and high amplitudes, scatter out thereby escaping from their holes. After this step, it was found that resin material using in 3D printing could not provide necessary stability for bubble propulsion. Nevertheless, to be definitely sure, thinner walled designs in which the bubble movements are easier to observe were constructed.

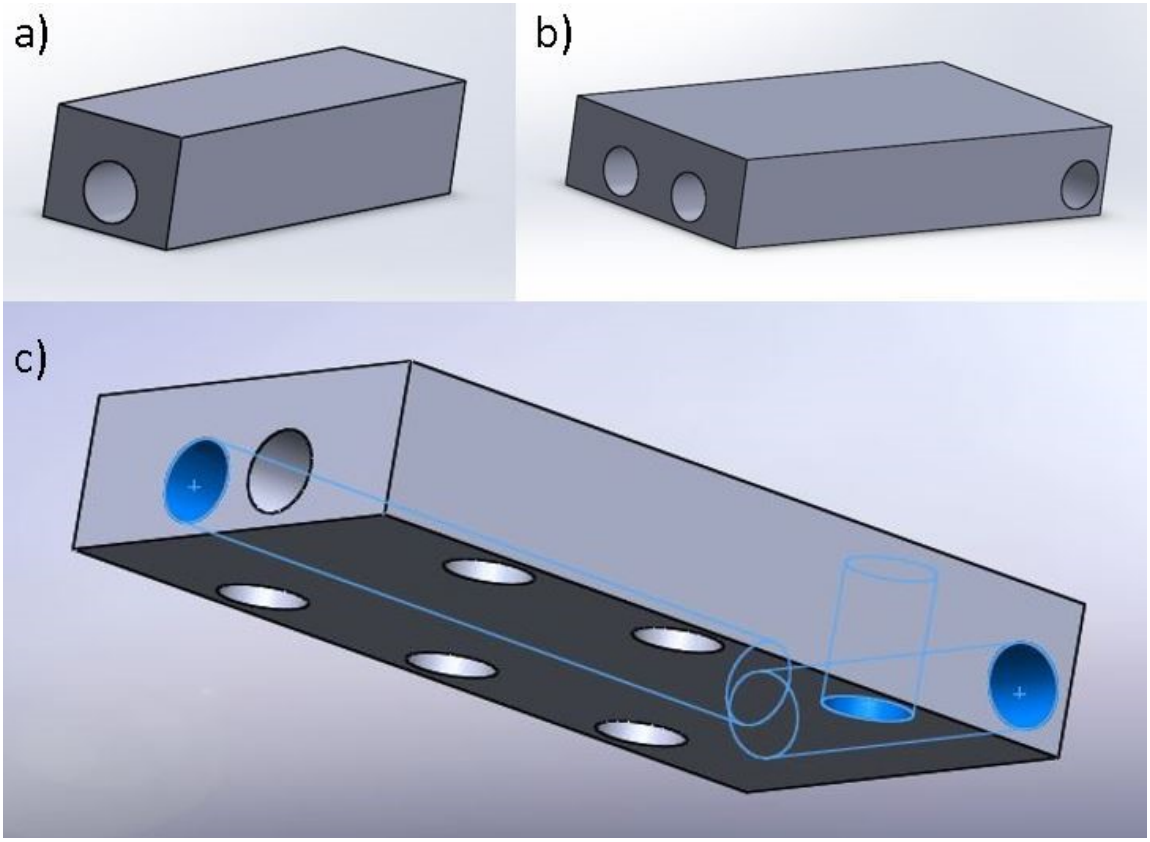

Figure 16: The Thin-walled Designs that made to observe the Bubble Oscillation and Movement inside of the Tube

All designs shown in the Figure 16 are built in different sizes and diameters, where the proper bubble oscillations were tried to be observed in tubes. This time in the experiment, the focus was only on the captured bubble oscillation regardless of the frequency calculation. Once again a wide frequency spectrum scanned with 100 Hz increments.

At very high voltages and several frequency values, the bubble inside the channel escaped by dividing into smaller bubbles. An article published in 2006, which mentions irregular behavior and weaker effect of sound wave was also observed in the resin

material [28]. The big bubble captured in the channel was observed to escape via dividing into smaller bubble parts. In this case the high amplitude values affects slightly the inner regions. Even in this case proper bubble oscillations cannot be observed. Since successful observations could not be made, we decided to change material with PDMS.

The PDMS was tested only for 1D motion. For this, a mold was prepared from 3D printer. The device required for the test was obtained by pouring liquid PDMS on the mold and cured. New PDMS device was tested in different low-high frequency at various amplitudes. However, the acoustic bubble cavitation and propelling effect have not observed. The bubbles were observed that escaping by dividing into bubble pieces that similarly occurred in the resin material based device testing.

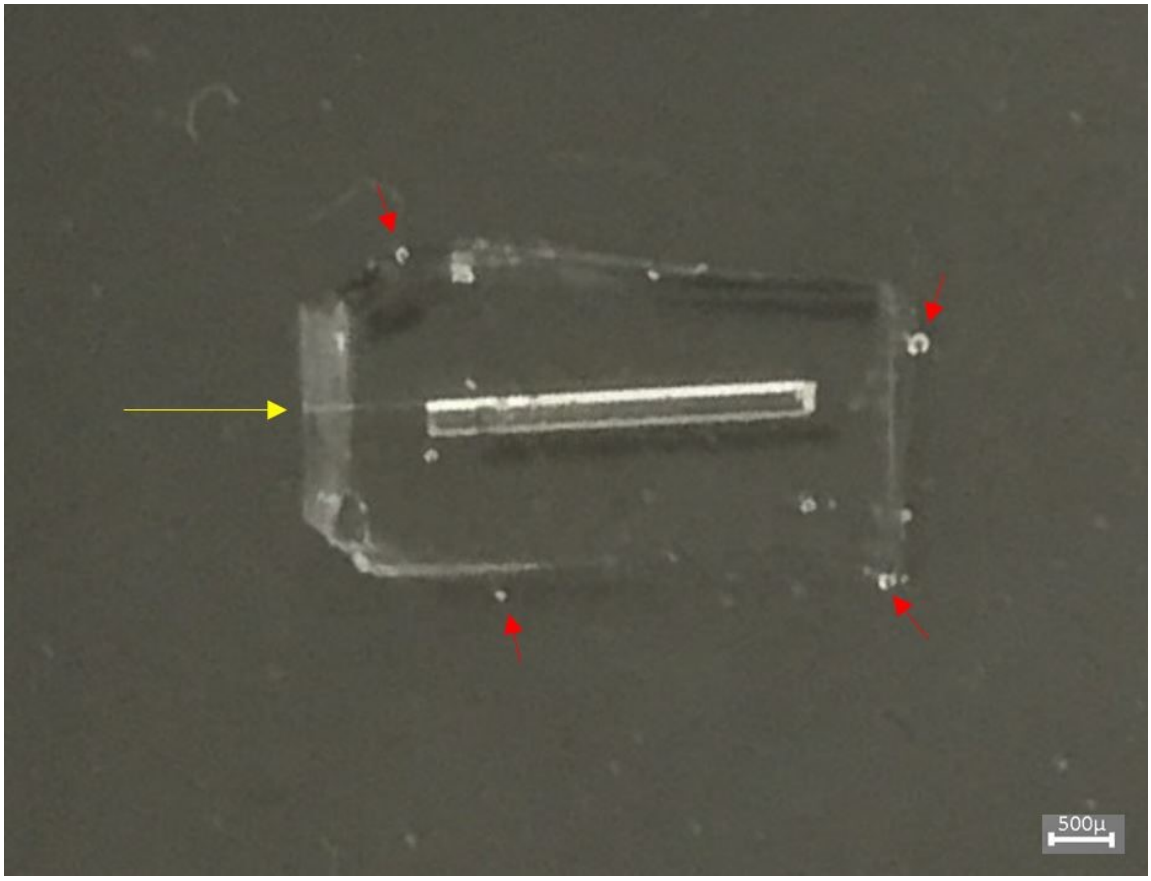

Figure 17: Captured Bubble Deformation and Small Bubbles Scattering

As it seen in the Figure 17, red arrows are some of the scattered bubbles from the captured bubble. The reduction of the bubble volume can be seen from the yellow arrow which shows the orifice of the device. The bubble trapped inside of the tube did not oscillate properly and divided into bubble pieces. In addition, in Figure 17, it is seen that many small parts of the bubble fled out from the tube orifice, and the smooth bubble structure has deformations inside of the tube.

According to the previous experiments, the acoustic wave causes an inconsistent behavior inside of the resin and PDMS channels. However, one of designs has worked.

From working point, we have created better designs and futuristic estimations for valuable application of bubble oscillation actuated device.

6.2. Designing, Testing and Results for Encapsulated Micro-Tube Bubble Propulsion

According to the previous section the working principles are captured bubble and its oscillation inside of the microchannel. However, this application is good for only few of materials such as parylene and Teflon according to the related researches [27, 28]. However, they are only have conventional microfabrication methods which are not suitable for complex designs. This research leads to create a way to use bubbles oscillation inside almost every kind of materials which have inconsistent reaction to the soundwave propagation and reflection. In this research, the used materials are generally PDMS and Resin based which are the most prevalent in soft MEMS and 3D printing applications [29-31]. The design different from all others has worked and the bubble has oscillated not inside but outside of the resin microchannel. It has oscillated at the orifice of the channel. Further, designs has started with this observation.

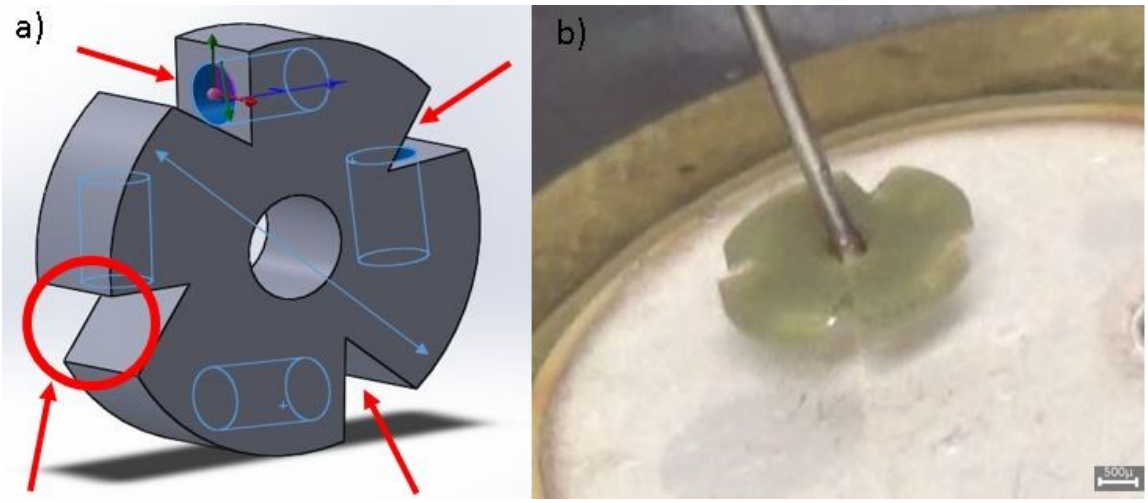

Figure 18: The First Worked Design

In the Figure 18, the captured bubbles inside of the microchannel come out and stay at the red arrows showed places. After than the oscillation of the bubbles becomes more consistent and crates propulsion effect, because with only this way bubbles can get an appropriate wave of sound for oscillation. According to the equation 2.6 the device bubble possibly oscillate at around 2.5 kHz. However, it has oscillated at 5.4 kHz 120 V_{pp} with 170 RPM. Lower voltage has achieved according to the latest work [27] in this field and faster. The previous work has 480 V_{pp} and 75 RPM. According to the equation 3.5 the oscillation frequency should be around 5 kHz which is relatively close to the experimental results.

Furthermore, there is an also sound field exposure time effect.[32] The exposure time can change a little the behavior of a bubble oscillation because the water and device temperature are increased.[33] In addition to temperature change, 3D printing structures has very tiny holes and steps when they are examined under a microscope. These steps

and holes can create a little inconsistency and step by step bubble oscillation motion. While a bubble oscillating, the steps and micro holes can affect the behavior of a bubble. Thus, in research the effect of a 3D printer operating resolution is investigated.

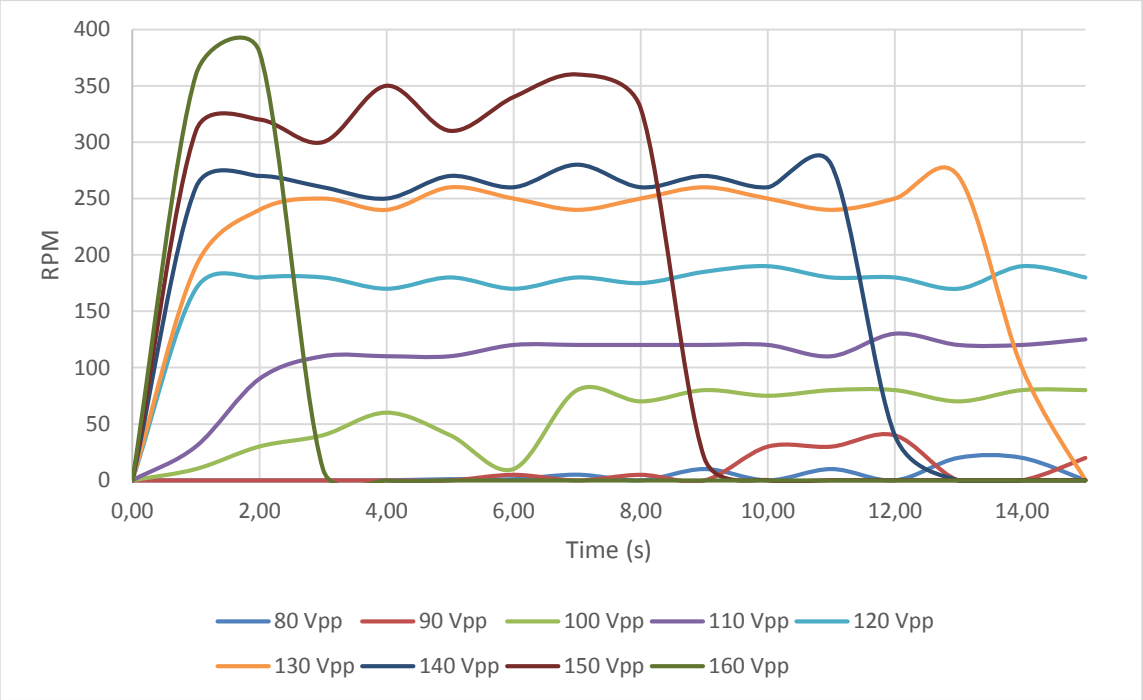

Figure 19: Sound Field Exposure Time Effect on a Spinning Device Speed and Operating Period

According to Figure 19, sound field exposure time has a significant effect on bubble actions inside of the device. Higher the amplitude makes lower the operating time of the device. To get an optimized effect and more testing time will give the device more reliability instead of having high speed turning effect.

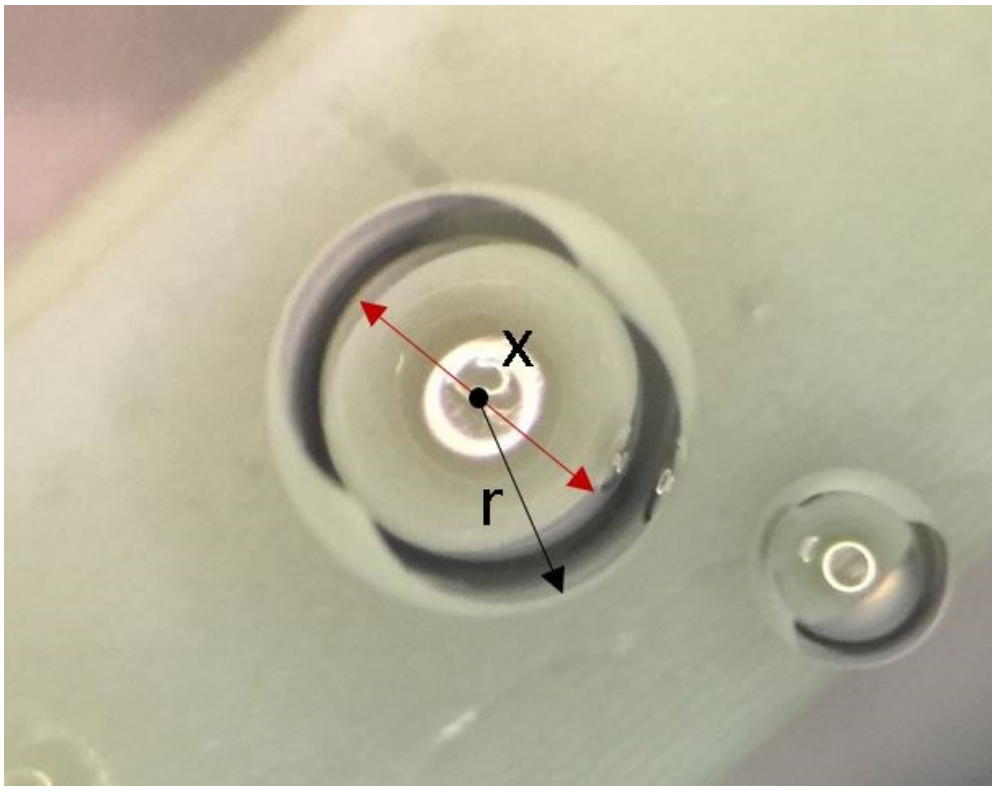

Figure 20: Determining the Bubble Contact Angle at Resin Material

To find out the contact angle of a bubble ad resin material, a bubble contacted to the surface of the resin layer observed. The contact points are determined, and with the reverse cosine the angle is calculated. As it seen in Figure 20, r is the radius of the bubble and x is the contact surface, which is circular shape, diameter. From the provided ratio between x and 2r and 3D sphere section calculation with basic geometry calculation. The contact angle of a bubble at resin material is 49°. To determine the adhesion force between bubble and solid surface we need to know the contact angle. Also this estimation gives an idea of a bubble size for oscillation frequency when the captured bubble comes out. However, the calculation of the sphere volume calculation with a contact angle changes do not give good idea about oscillation frequency in terms

of experimental. However, the calculation of captured bubble volume frequency estimation is better than a contact angle affected bubble oscillation frequency estimations in terms of the changes at bubble radius.

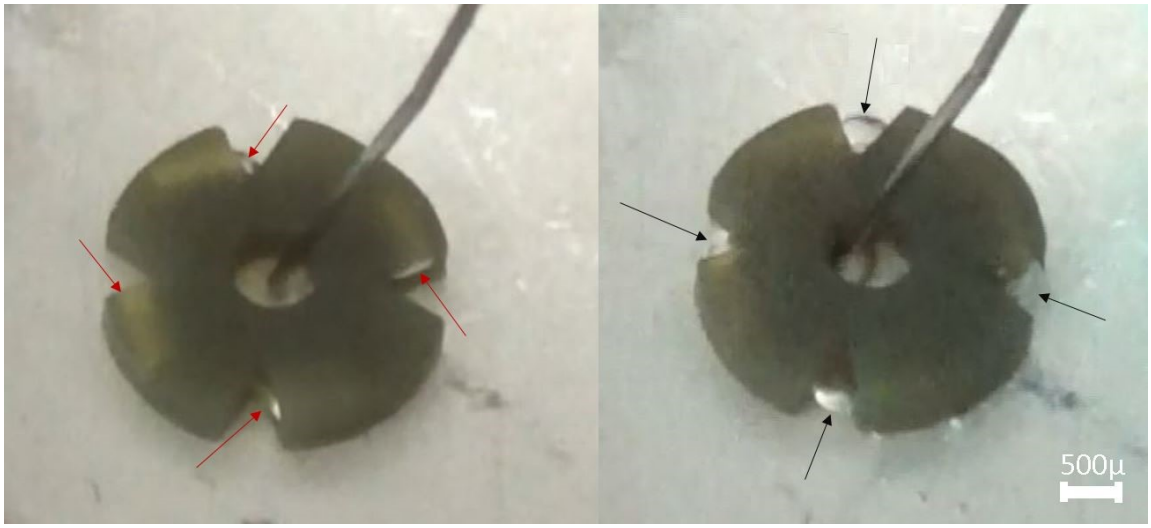

Figure 21: Captured Bubbles and Locked Bubbles

Bubbles are captured when the design throws or puts in the liquid media same as Figure 21 that showed by a red arrows. The captured bubbles in the tube oscillates and comes out because of the length of a trapped bubble is not too long to divide into pieces. However, the sound is strong enough to take of the bubble from the tube. When the bubbles come out, they are blocked by the additional blocks. These blocks do not let the bubble run away at certain level of sound wave amplitude. The blocked bubbles have contact surfaces on the design surfaces. These contacts represent amount of adhesion force while bubbles are oscillating. The bubbles oscillation creates force against to the adhesion force, and creates push effect. According to the surface adhesion force

calculation on inner surface of the tube shows this effect can be higher in high shear strain rated materials.

In addition to, the design is printed several times by 3D printer. However, newer designs were not oscillating properly and even oscillation occurs at the spinning device were under 60% of its previous turning effect performance. Same designs that printed in different time are observed under the microscope. According to the observation two device were same by their shapes but they were not the same in terms of smooth structure.

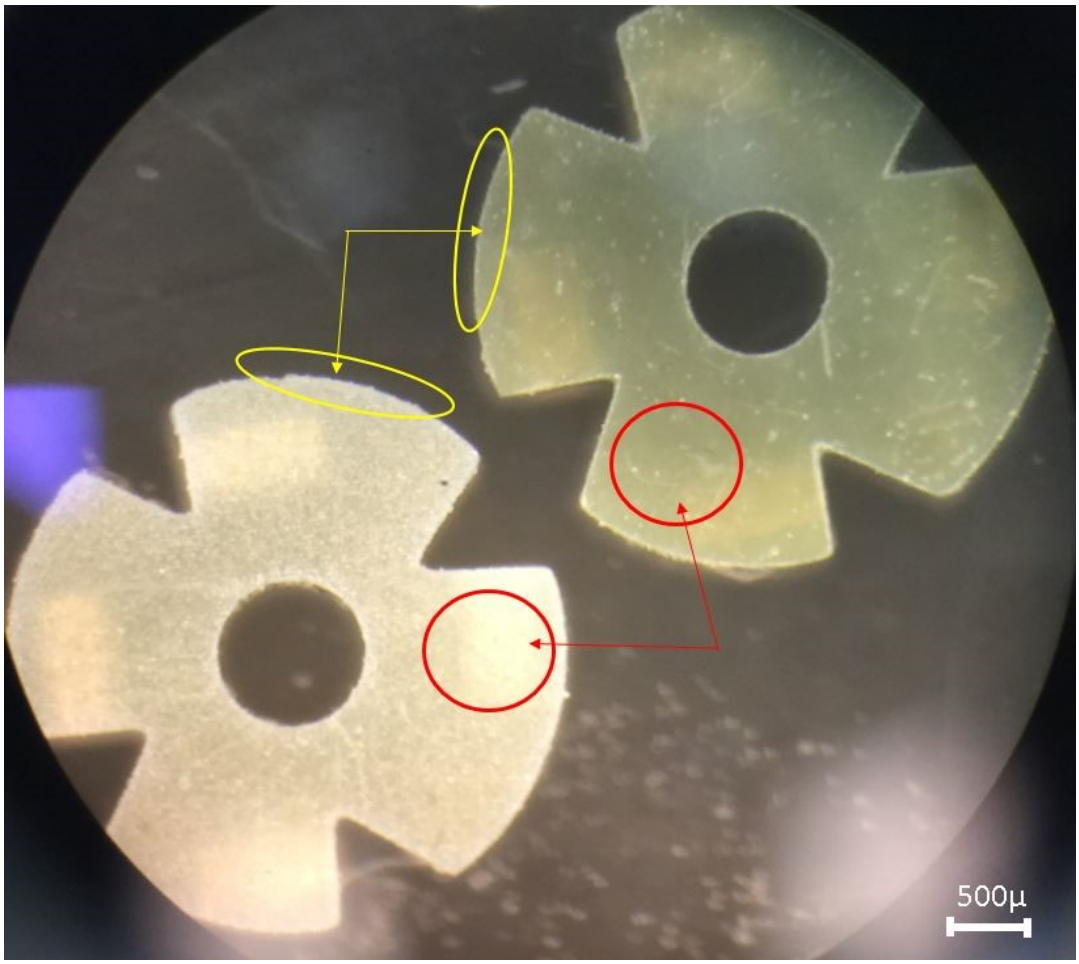

Figure 22: Same Devices in Different Printing Time Period

As it seen from Figure 22 the devices have same dimensions and designs. However, their surface smoothness, which is shown by red circle, and corner resolutions, which is shown by yellow ellipse, are different. Right hand side designed is worked 2-3 times better in terms of RPM speed. After having research on this problem, the differences in smoothness and quality are caused by the 3D printer exposure time increased. More exposure time means that more cured which has some very tiny micron gaps in the material and lower liquid density. According to the weight measurement of the devices, right hand side one is 11 mg, and the left one is 7 mg. These results are supported the prediction. After changing the exposure time the problem has solved. By the way, the problem is also shown that lower resolution printers will not work efficiently and properly according to the stereolithography ones. Even a stereolithography technique based printer can be used, the exposure time should optimize to get better and satisfying results. Several designs have achieved and tested for various applications.

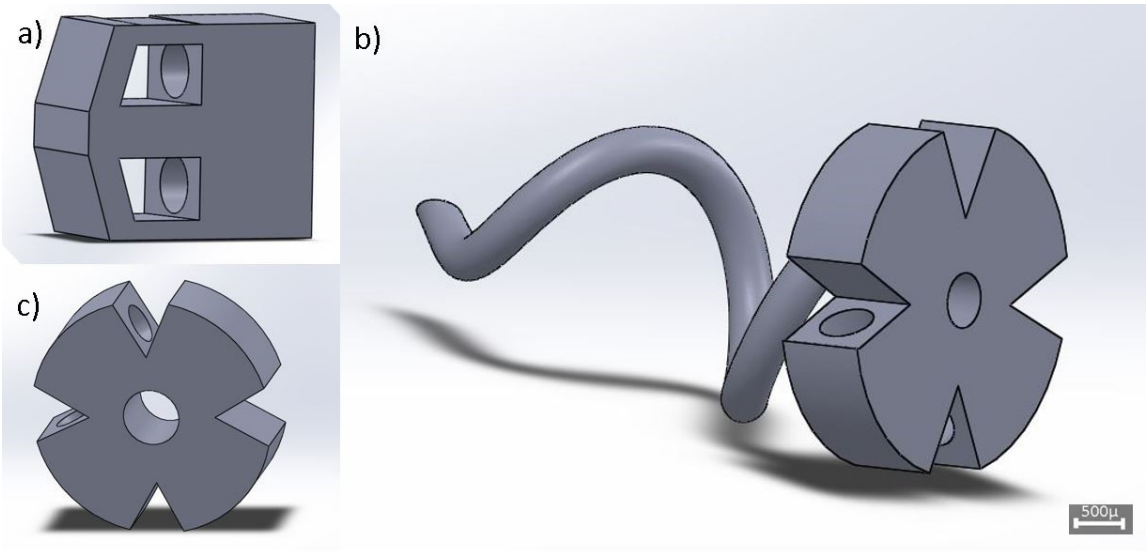

Figure 23: a) The propulsion device, b) Rotational device to create cork screw motion for viscous fluids, c) Smaller spinning device.

In the Figure 23 a), the device moves one direction with applied acoustic wave at 4.5 kHz and 157 V_{pp}. The design in the Figure 23 b) represents a new approach to a rotational movement for higher viscous fluids. Cork screw motion is a method to overcome scallop effect [15, 16]. In addition to other designs, a smaller design which is in figure 23 c) performed and tested. According to the results, the smaller design operated at higher frequency than the first spinning device.

As it seen from the figure 23, printing designs are unlimited by 3D printers. The printing resolution of the 3D printer is around 30 µm. With owing better resolution 3D printers it is possible to create a smaller device with using the same structural phenomena.

From the spinning device, many additional testing have been made. According to the experiences, acoustic wave effect on swimmers tried to be understood. The first testing

was determining the spinning device bubble oscillation frequency change by the changes in hydrostatic pressure. Oscillation frequency of bubbles and RPM of the device are determined by increasing the level of water in the testing vessel.

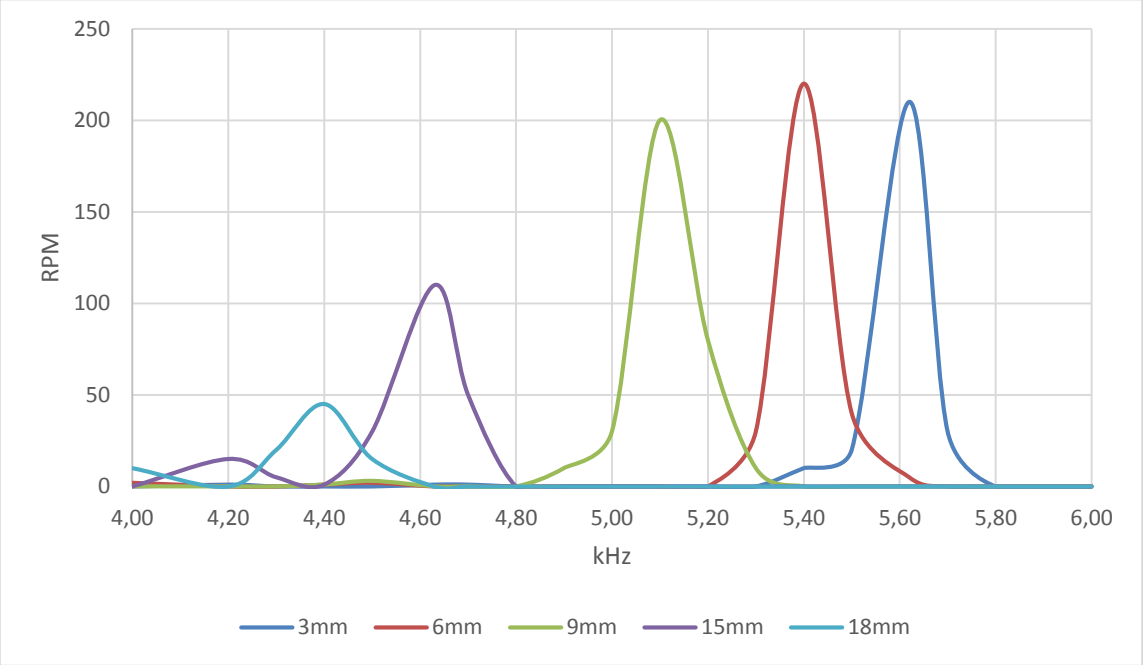

Figure 24: Bubble Oscillation Frequency and Device RPM Changes in Vessel by Changing the Liquid Level

According to the results in Figure 24, higher hydrostatic pressure reduces the oscillation frequency of bubble in spinning device. Rotation speed also changes with the hydrostatic pressure because of the changes at bubble activity.

Furthermore, the effect of sound wave blocked by a layer was tested, and the oscillation frequency on the device was also observed.

Layer Material	Layer Thickness	Oscillation Amplitude
Resin	1 mm	320 Vpp
Glass	1 mm	490 Vpp
Pyrex	1 mm	>>500 Vpp
PDMS	1 mm	240 Vpp
Polystyrene	1 mm	130 Vpp

Table 2: Layer Blocking Effect on Spinning Device

According to the Table 2, attenuation and reflection are the main issue of sound wave propagation through the spinning device. Oscillation of the bubbles in the device has observed in several amplitudes. However, pyrex and glass were the lowest impact at the oscillation. Polystyrene layer had the highest transitive effect on soundwave and device has worked regularly. Also, reduction at the spinning speed was notable exclusively polystyrene layer. Accordingly, using a polystyrene base container can be better choice for testing. However, testing should be in the liquid media and

In addition to all experiment, the effect of the distance change from the center of piezoelectric transducer without making any other changes is tested. Water temperature and level are kept stable. Only the distance of the spinning device from the transducer was changed.

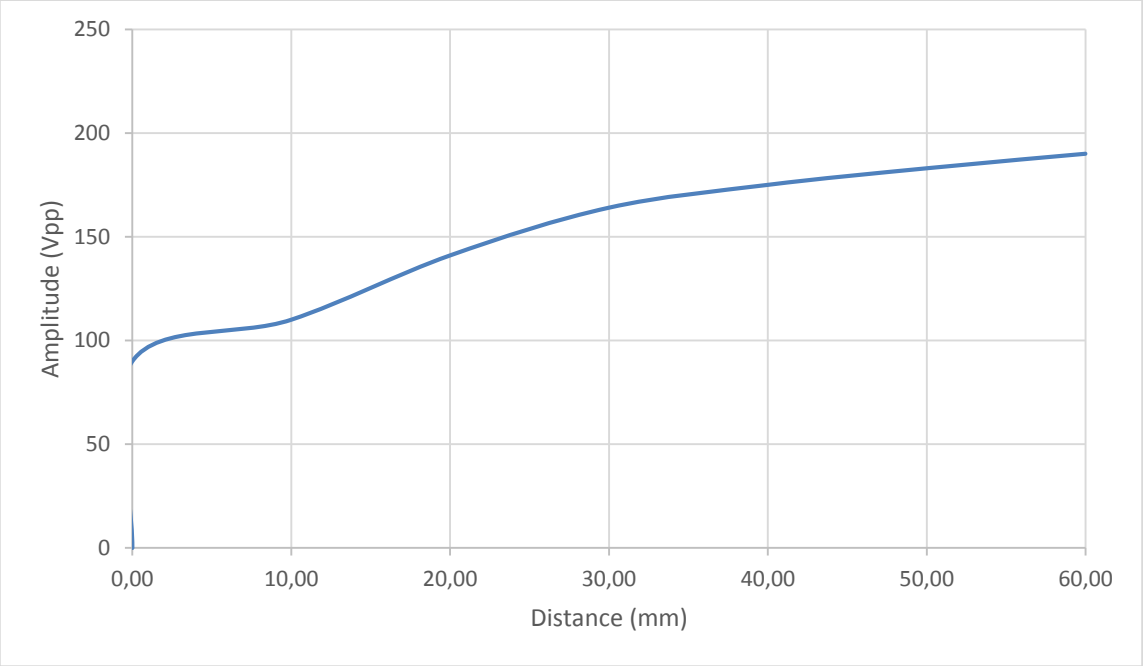

Figure 25: Applied Sound Wave Amplitude Changes by Distance of the Device from the Center of Piezoelectric Transducer

According to the graph in Figure 25, pulling away the spinning device from the sound source requires signal amplification. The applied frequency was not changed in the meanwhile.

The spinning device can be used in many applications such as mixing, switching, actuating and so forth. The device is tested as a mixer to demonstrate how effective and valuable for microfluidic purposes.

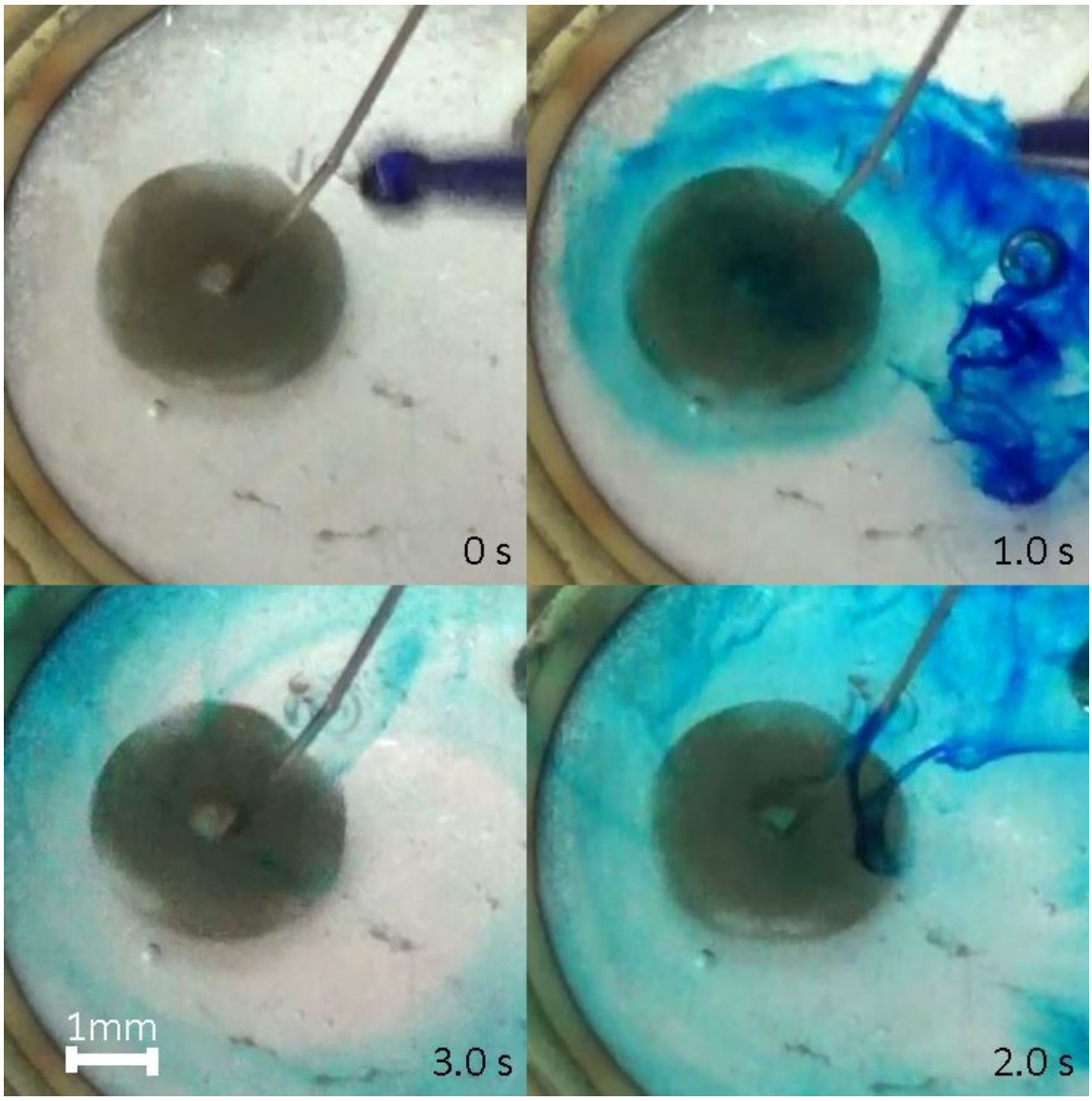

Figure 26: Spinning Device Fast Mixing Ability Time by Time

The spinning device represent its valuable and fast ability at mixing food dye in the Figure 26. 2 mm in radius device that is actuated by small microbubbles is achieved. The device had speed around 400 RPM. A whirl was created. The active mixing area was approximately 18 mm in diameter. The mixing efficiency by the distance has also

examined and observed. The bubbles captured in the mixing device has also generated 3.4 x 10^{-9} Nm as a torque with disregarding the friction.

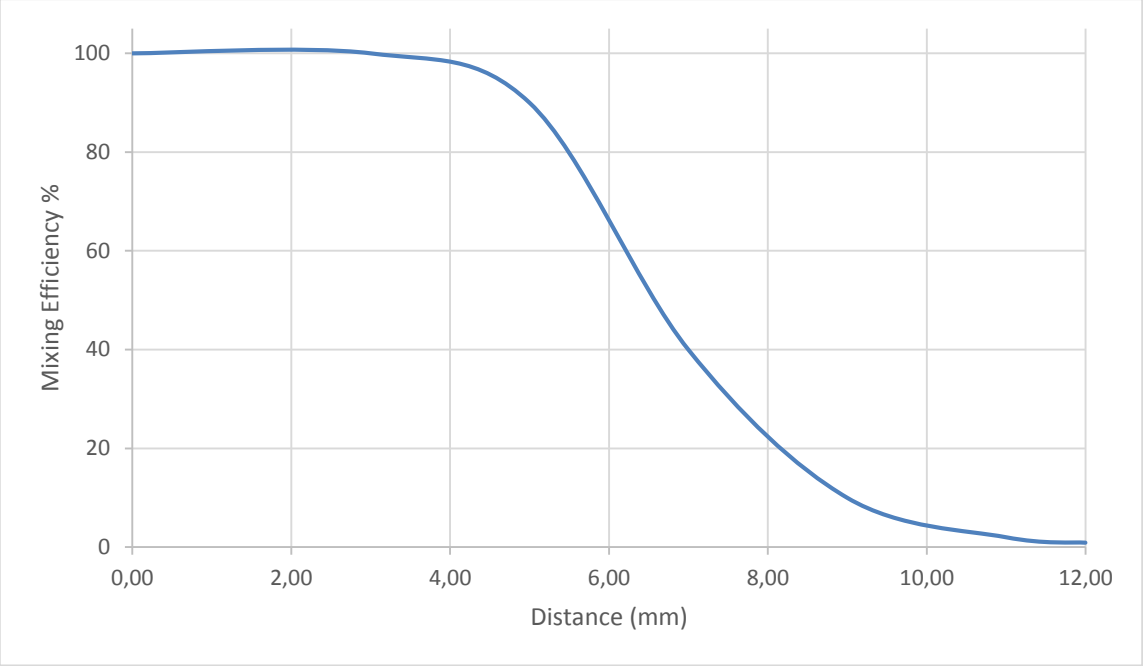

Figure 27: Mixing Efficiency of the Device vs Distance from Center of the Mixer

As it seen in Figure 27, the mixing capability is the highest in the circular area of 4 mm in radius. According to the fast rotational characteristic of the device, it is valuable for further implementations and MEMS applications. The effective area of mixing device is around 200 mm^2. The mixing effect is valuable in terms of implementing the device into microfluidic channel. However, laminar flow and turbulent flow patterns should be investigated. The device and bubble respond to the flow rate has to minimize with better implementation ideas and techniques. The video of mixing is provided as a supplementary video file in mp4 format.

In addition to spinning device, also bubble pushing device is designed and tested.

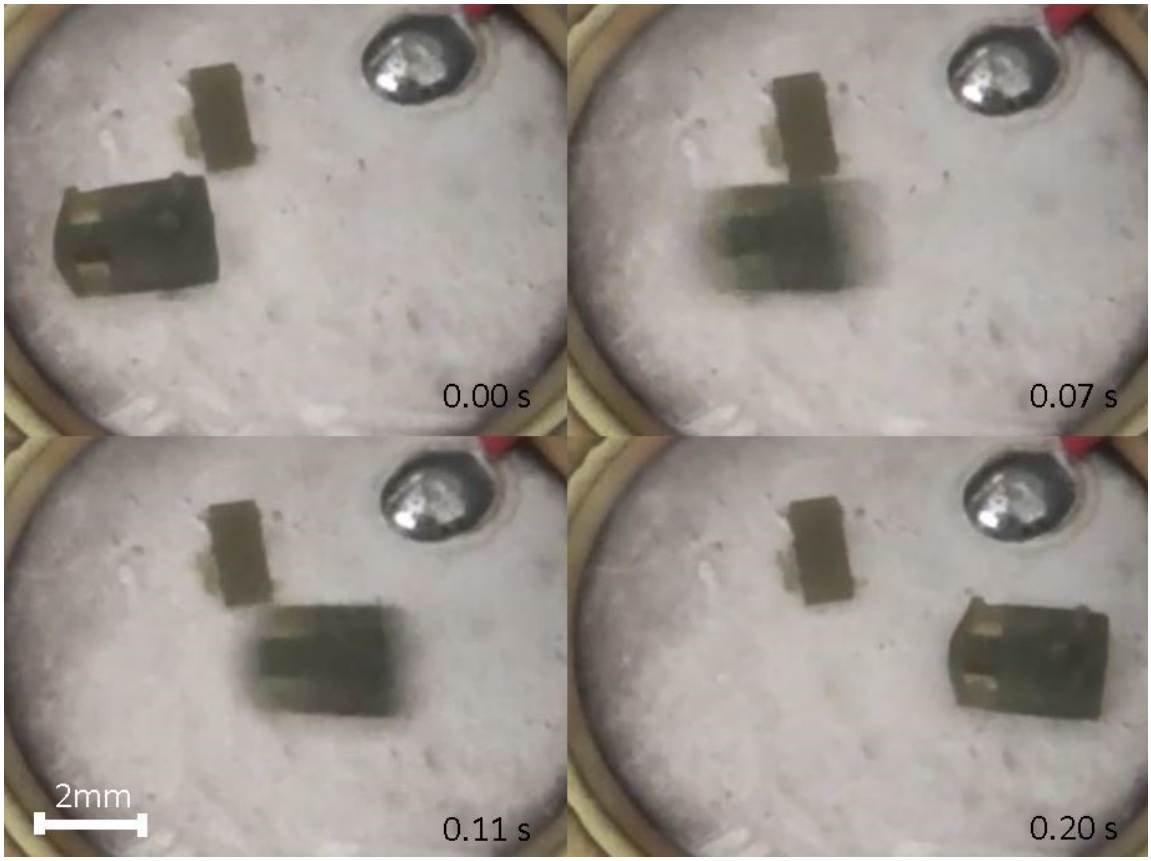

Figure 28: Fast Push Effect of Acoustic Bubble Actuated Device in a Few Split Seconds

The acoustic bubble pushing device is achieved. The device length is 3.3 mm. The device speed was around 600 BPM which equals to 33 mm/s. As it seen in the Figure 28, the captured bubble oscillation creates a fast push effect on the device. The video of the push effect device is provided as a supplementary mp4 format video file.

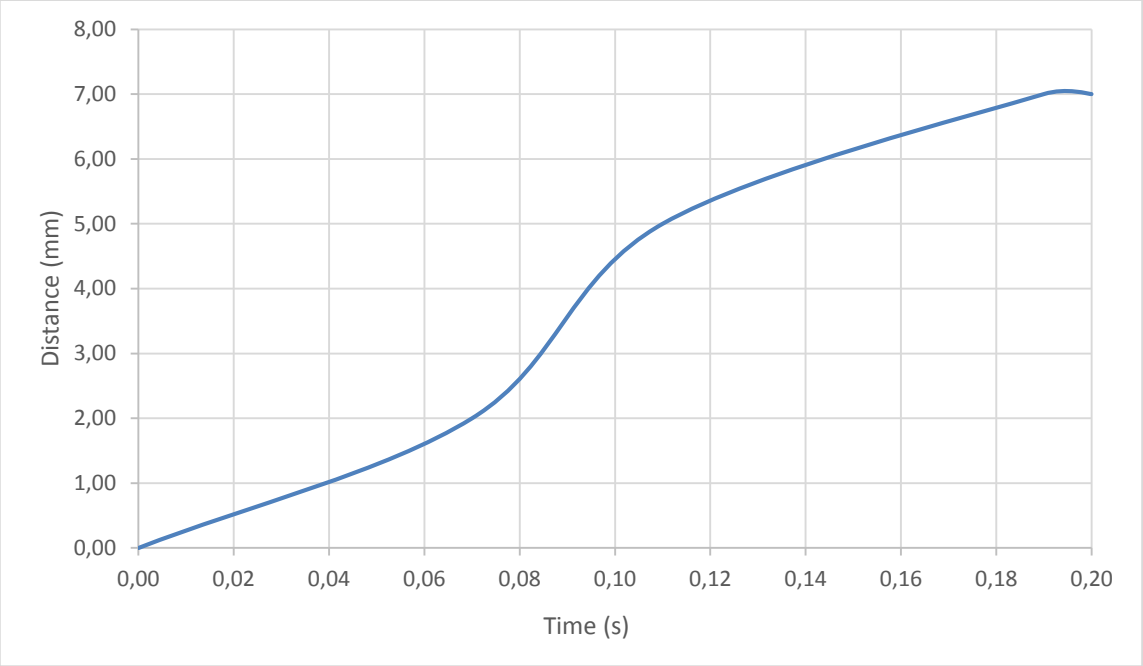

Figure 29: The Distance vs Time Graph of the Push Effect Device

From the Figure 29, the average speed of the device is achieved 33 mm/s. The results are made the design valuable in terms of propulsion speed. However, low Reynolds numbers should also investigate to compare to all propelling and push effect devices in literature.

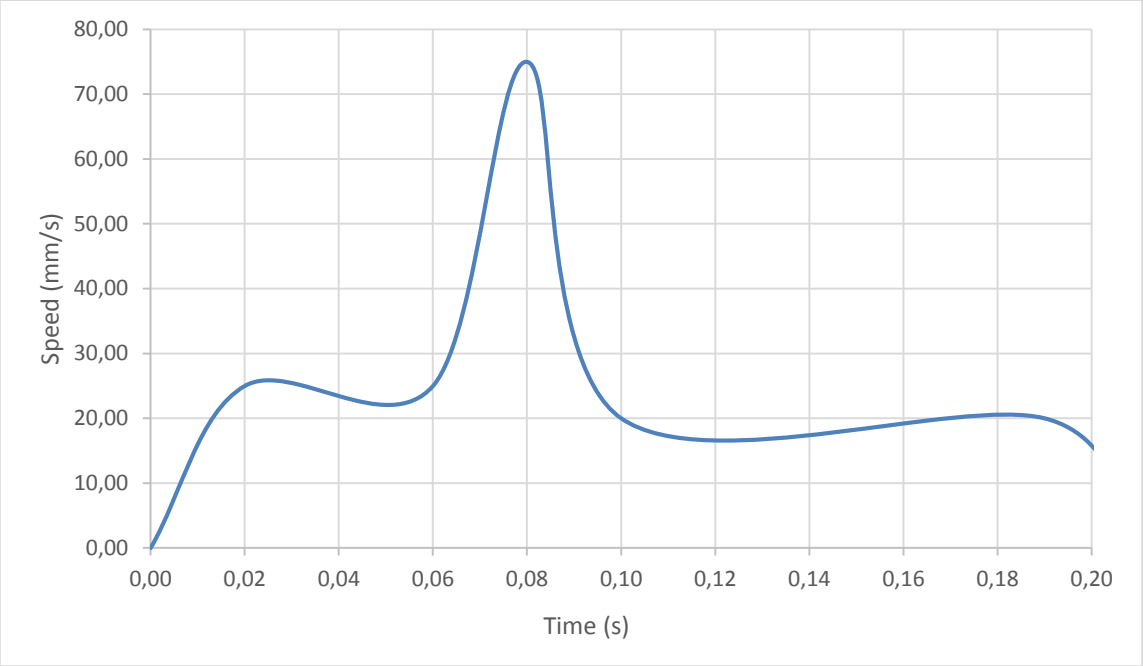

Figure 30: Speed vs Time Fast Push Effect Bubble Actuated Device

According to the Figure 30, there is a significant speed peak between 0.06 and 0.10 seconds. The peak is caused by the reduction of friction of the device at the piezoelectric transducer center part. Friction is lowered by the highest vibration (expanding and narrowing behavior) occurrence in the middle of the transducer. The design weight is around 8 mg. According to the acceleration and mass with the motion the maximum force without counting the surface friction is around 20 $x10^{-6}$ N.

The successful results of the fast push effect device is motivated us to design 2D and 3D moving and pushing devices. In addition, the device is also motivated us to consider the usage at micro surgery and/or other medical purposed applications in the near future.

The additional designs for testing environment such as holding the rotational devices, other fabrication mold pictures are given at Appendix A. The experiment setup and other real device photos are given at Appendix A.

7. SUMMARY AND FUTURE WORK

7.1 Summary

Acoustically oscillated bubbles are interesting in MEMS applications in terms of various oscillation frequency abilities. Therefore, different sized bubbles are tried to capture by researchers inside of a tube outside of a device and so forth. However, this study is unique in terms of capturing bubble in tube and keeping it at near of the orifice of a tube. Keeping a bubble with restriction by using a blockage creates a returning and expending behavior through the tube. This behavior creates a propulsion effect because of the bubble external part having interaction surface with the inner surface of the tube itself. The interaction creates a force while expending shrinking effect of the bubble and changing bubble boundary shape very fast. In this situation, the bubble creates a surface force, and adhesion force creates reverse force to the surface force. The forces interactions creates propelling effect through the end of the channel. A device can be actuated by this phenomena.

Effectively spinning and propelling effect are achieved. These effects are easy to use in any non-contact applications.

7.2 Future Work

The future works areas are very broad because of the effectiveness of the designs and their characteristics. The unique designing technique gives an opportunity to perform any kind of movement in microfluidics with bubble oscillation. Bubble actuated 3D moving devices can be fabricated easily by 3D printers. Therefore, this work becomes more valuable than any other competitors. With the technological

developments in 3D printing industry create potential futuristic designs. More feasible and more effective few micron scale devices can be fabricated for any kind of contactless applications. Testing and optimizing newer designs by printing higher resolution few micron scale printers can be tested and searched. Also switching oscillation frequencies of different sized captured bubbles to manipulate a device to operate different directions can be tested and performed. In addition to, to avoid scallop effect of a device in microfluidics, cork screw motion ability can be implemented into a design to overcome.

In future with optimization of bubble oscillation in veins, micro surgery can be performed by driving the bubble oscillation based surgery device with acoustic wave while observing it with ultrasound imaging machine.

REFERENCES

[1] T. Mei, Y. Chen, G. Fu, and D. Kong, "Wireless drive and control of a swimming microrobot," in *Robotics and Automation, 2002. Proceedings. ICRA'02. IEEE International Conference on*, 2002, pp. 1131-1136.

[2] D. J. Bell, S. Leutenegger, K. Hammar, L. Dong, and B. J. Nelson, "Flagella-like propulsion for microrobots using a nanocoil and a rotating electromagnetic field," in *Robotics and Automation, 2007 IEEE International Conference on*, 2007, pp. 1128-1133.

[3] P. Tierno, R. Golestanian, I. Pagonabarraga, and F. Sagués, "Magnetically actuated colloidal microswimmers," *The Journal of Physical Chemistry B,* vol. 112, pp. 16525-16528, 2008.

[4] A. Snezhko, M. Belkin, I. Aranson, and W.-K. Kwok, "Self-assembled magnetic surface swimmers," *Physical Review Letters,* vol. 102, p. 118103, 2009.

[5] W. Gao, A. Uygun, and J. Wang, "Hydrogen-bubble-propelled zinc-based microrockets in strongly acidic media," *Journal of the American Chemical Society,* vol. 134, pp. 897-900, 2011.

[6] A. A. Solovev, Y. Mei, E. Bermúdez Ureña, G. Huang, and O. G. Schmidt, "Catalytic microtubular jet engines self-propelled by accumulated gas bubbles," *Small,* vol. 5, pp. 1688-1692, 2009.

[7] A. Laskar, R. Singh, S. Ghose, G. Jayaraman, P. S. Kumar, and R. Adhikari, "Hydrodynamic instabilities provide a generic route to spontaneous biomimetic oscillations in chemomechanically active filaments," *Scientific Reports,* vol. 3, 2013.

[8] B. Behkam and M. Sitti, "Bacterial flagella-based propulsion and on/off motion control of microscale objects," *Applied Physics Letters,* vol. 90, p. 023902, 2007.

[9] R. Dreyfus, J. Baudry, M. L. Roper, M. Fermigier, H. A. Stone, and J. Bibette, "Microscopic artificial swimmers," *Nature,* vol. 437, pp. 862-865, 2005.

[10] A. Najafi and R. Golestanian, "Propulsion at low Reynolds number," *Journal of Physics: Condensed Matter,* vol. 17, p. S1203, 2005.

[11] P. Hänggi and F. Marchesoni, "Artificial Brownian motors: Controlling transport on the nanoscale," *Reviews of Modern Physics,* vol. 81, p. 387, 2009.

[12] H.-R. Jiang, N. Yoshinaga, and M. Sano, "Active motion of a Janus particle by self-thermophoresis in a defocused laser beam," *Physical Review Letters,* vol. 105, p. 268302, 2010.

[13] J. Gibbs and Y. Zhao, "Autonomously motile catalytic nanomotors by bubble propulsion," *Applied Physics Letters,* vol. 94, p. 163104, 2009.

[14] J. Vicario, R. Eelkema, W. R. Browne, A. Meetsma, R. M. La Crois, and B. L. Feringa, "Catalytic molecular motors: fuelling autonomous movement by a surface bound synthetic manganese catalase," *Chemical Communications,* pp. 3936-3938, 2005.

[15] E. M. Purcell, "Life at low Reynolds number," *Am. J. Phys,* vol. 45, pp. 3-11, 1977.

[16] S. K. Cho, "Mini and micro propulsion for medical swimmers," *Micromachines,* vol. 5, pp. 97-113, 2014.

[17] J. Wang, *Nanomachines: Fundamentals and Applications*: John Wiley & Sons, 2013.

[18] T. Leighton, *The Acoustic Bubble*: Academic Press, 2012.

[19] P. N. T. Wells, *Biomedical Ultrasonics*: Academic Press, 1977.

[20] C. Glorieux, K. Van de Rostyne, V. Gusev, W. Gao, W. Lauriks, and J. Thoen, "Nonlinearity of acoustic waves at solid–liquid interfaces," *The Journal of the Acoustical Society of America,* vol. 111, pp. 95-103, 2002.

[21] H. Medwin and C. Clay, "Fundamentals of acoustical oceanography academic," *New York,* pp. 11-12, 1998.

[22] M. Minnaert, "XVI. On musical air-bubbles and the sounds of running water," *The London, Edinburgh, and Dublin Philosophical Magazine and Journal of Science,* vol. 16, pp. 235-248, 1933.

[23] H. Oguz and A. Prosperetti, "The natural frequency of oscillation of gas bubbles in tubes," *The Journal of the Acoustical Society of America,* vol. 103, pp. 3301-3308, 1998.

[24] J. McFarlane and D. Tabor, "Adhesion of solids and the effect of surface films," in *Proceedings of the Royal Society of London A: Mathematical, Physical and Engineering Sciences*, 1950, pp. 224-243.

[25] J. Feng and S. K. Cho, "Micro propulsion in liquid by oscillating bubbles," in *Micro Electro Mechanical Systems (MEMS), 2013 IEEE 26th International Conference on*, 2013, pp. 63-66.

[26] J. Feng and S. K. Cho, "Two-dimensionally steering microswimmer propelled by oscillating bubbles," in *Micro Electro Mechanical Systems (MEMS), 2014 IEEE 27th International Conference on*, 2014, pp. 188-191.

[27] J. Feng, J. Yuan, and S. K. Cho, "Micropropulsion by an acoustic bubble for navigating microfluidic spaces," *Lab on a Chip,* vol. 15, pp. 1554-1562, 2015.

[28] R. Dijkink, J. Van der Dennen, C. Ohl, and A. Prosperetti, "The 'acoustic scallop': a bubble-powered actuator," *Journal of Micromechanics and Microengineering,* vol. 16, p. 1653, 2006.

[29] H. Takao, K. Miyamura, H. Ebi, M. Ashiki, K. Sawada, and M. Ishida, "A MEMS microvalve with PDMS diaphragm and two-chamber configuration of thermo-pneumatic actuator for integrated blood test system on silicon," *Sensors and Actuators A: Physical,* vol. 119, pp. 468-475, 2005.

[30] J. Streque, A. Talbi, P. Pernod, and V. Preobrazhensky, "New magnetic microactuator design based on PDMS elastomer and MEMS technologies for tactile display," *Haptics, IEEE Transactions on,* vol. 3, pp. 88-97, 2010.

[31] T. Ninomiya, Y. Okayama, Y. Matsumoto, X. Arouette, K. Osawa, and N. Miki, "MEMS-based hydraulic displacement amplification mechanism with completely encapsulated liquid," *Sensors and Actuators A: Physical,* vol. 166, pp. 277-282, 2011.

[32] M. Campbell, J. Cosgrove, C. Greated, S. Jack, and D. Rockliff, "Review of LDA and PIV applied to the measurement of sound and acoustic streaming," *Optics & Laser Technology,* vol. 32, pp. 629-639, 2000.

[33] M. P. Da Cunha, T. Moonlight, R. Lad, G. Bernhardt, and D. Frankel, "P4L-1 enabling very high temperature acoustic wave devices for sensor & frequency control applications," in *Ultrasonics Symposium, 2007. IEEE*, 2007, pp. 2107-2110.

APPENDIX A

The spinning device holder, microfluidic device designs and picture of the testing setup.

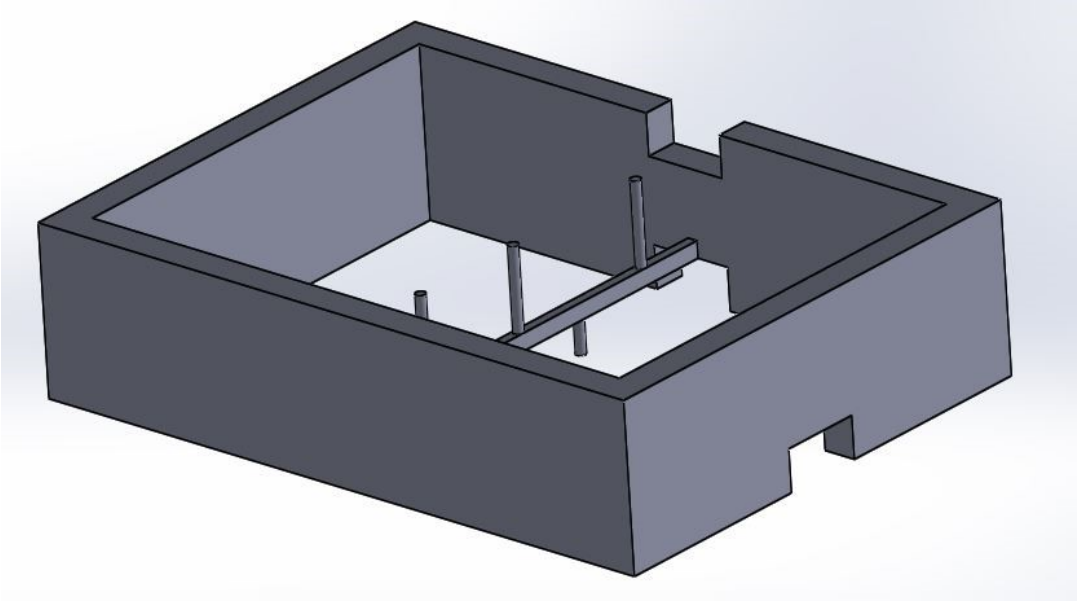

Figure A-1: The Spinning Device Holder and Testing Pool

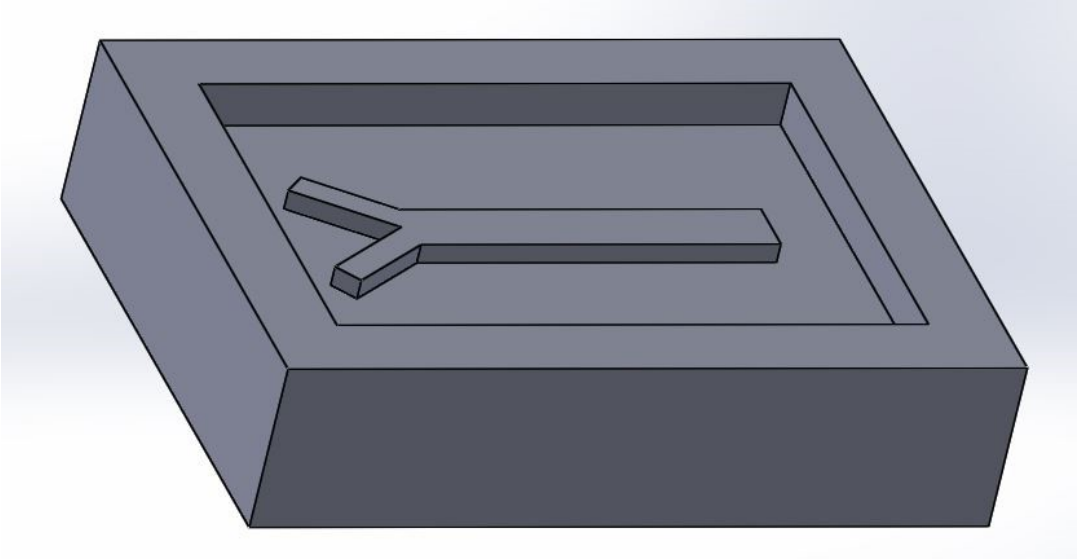

Figure A-2: The Mold Design for Microfluidic Channel for Liquid Mixing Design

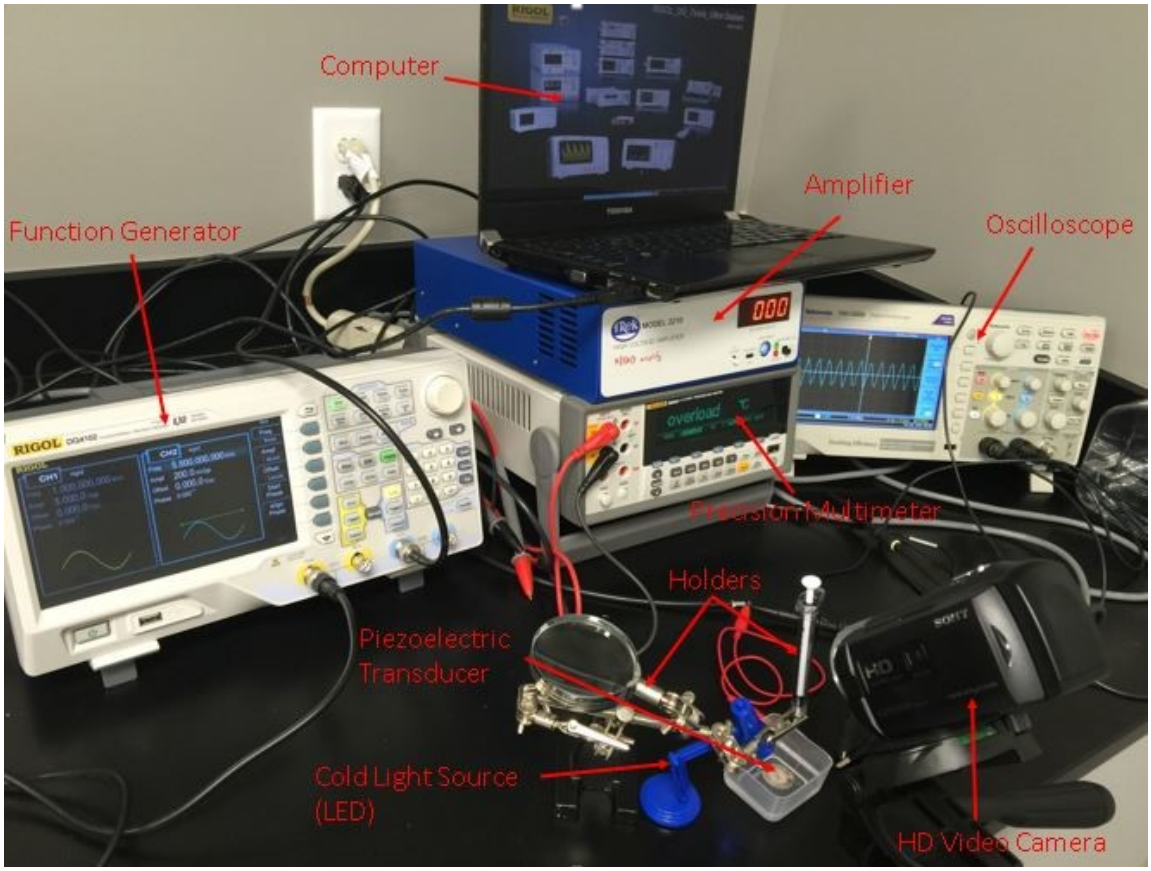

Figure A-3: Experimental Setup for Spinning and Jetting Devices

APPENDIX B

MATLAB codes are given below for the simulation that an acoustic wave propagation into water media is tested and observed theoretically;

```
close all; clear all;clc;
addpath functions
load Synthetic_data
[nz,nx] = size(velocityModel);
dx = 10; dz = 10;
x = (1:nx)*dx;  z = (1:nz)*dz;
subplot(131);imagesc(x,z,velocityModel);
xlabel('Distance (mm)'); ylabel('Depth (mm)'); title('Velocity Model');
hold on; hshot = plot(x(1),z(1),'w*'); hold off
colormap(seismic)
%% Create shot gathers
dt = min(min(dz./velocityModel/sqrt(2))); %time step
vmin = min(velocityModel(:));
nt = round(sqrt((dx*nx)^2 + (dz*nx)^2)*2/vmin/dt + 1); %time samples
t  = (0:nt-1).*dt; % total travel time
V = [repmat(velocityModel(:,1),1,10) velocityModel
repmat(velocityModel(:,end),1,10)];
V(end+1:end+10,:) = repmat(V(end,:),10,1);
```

```
f  = 20; % frequency
%% Generate shots and save to file and video
data = zeros(size(nt,nx));
figure(gcf)
for ixs = 3:nx+2
   rw = ricker(f,nz+2,dt,dt*ixs,0);
   rw = rw(1:nz,:);

   set(hshot,'XData',x(ixs-2),'YData',z(1));
   subplot(132)
   imagesc(x,z,rw(3:end-2,3:end-2))
   xlabel('Distance (um)'); ylabel('Depth (um)');
   title(['Shot ',num2str(ixs-2),' at ',num2str(x(ixs-2)),'um']);
   colormap(seismic)
   tic
   [data,snapshot] = fm2d(V,rw,nz,dz,nx,dx,nt,dt);
   toc
   if ismember(ixs-2,[1 nx/2 nx])
      start = 1;
   else
      start = nt;
   end
```

```
    for i = start:nt
        subplot(133); imagesc(x,z,snapshot(3:end-2,3:end-2,i))
        xlabel('Distance x (100um)'), ylabel('Distance y (100um)')
        title(['Wave Propagation t = ',num2str(t(i),'%10.3f')]); caxis([-0.14 1])
        drawnow;
    end
end
```